nature communications

Article

https://doi.org/10.1038/s41467-026-74574-z

Multiplexed cytokine and antigen mRNA administration generates durable anti-tumor immunity against pancreatic cancer

Received: 24 July 2025

Accepted: 9 June 2026

Published online: 19 June 2026

Check for updates

Chaitanya N. Parikh[1], Kelly D. DeMarco[1], Nikita Bhalerao[2], Hadiya K. Giwa[1], Griffin I. Kane[3], Ronnie W. Dinnell[3], Boyang Ma[1], Haruka Mori[1], Meghan L. Brassil[1], Katherine C. Murphy[1], Zhen Zhao[4,5], Calvin Johnson[2], Shriram Ramani[6], Lin Zhou[1], Loretah Chibaya[1], Youwei Qiao[7], Kai Hu[1], Lihua Julie Zhu[1,8,9], Brian C. Lewis[1,10,11], Wen Xue[7], Jason R. Pitarresi[2], Prabhani U. Atukorale[3,6,10] & Marcus Ruscetti[1,10,12]

Immunotherapy has limited success in pancreatic ductal adenocarcinoma (PDAC) due to an immune exclusive tumor microenvironment (TME) that lacks many cytokines necessary for Natural Killer (NK) and T cell responses. Here, we design multiplexed mRNAs encoding interleukins, chemokines, and interferons as a safe and effective cytokine therapy for PDAC. Intratumoral injection of IL-12, IL-18, CCL5, CXCL10, and IFNβ mRNAs achieves robust yet transient cytokine expression, leading to NK and $CD8^+$ T cell activation and reduced tumor growth and fibrosis in PDAC transplant mouse models. Combining cytokine with tumor antigen mRNAs enhances dendritic cell antigen presentation and $CD8^+$ T cell priming locally and systemically that prolongs animal survival after a single dose. Remarkably, nanoparticle encapsulation of the cytokine/antigen mRNA cocktail allows systemic administration and local delivery to autochthonous PDAC tumors in mice, culminating in curative responses in 50% of animals and antigen-reactive T cell persistence. These results suggest that multiplexed mRNA approaches to deliver cytokines and antigens generally absent in the TME could pave the way for effective immunotherapy in PDAC.

Pancreatic ductal adenocarcinoma (PDAC) is a highly aggressive malignancy with a median 5-year survival rate of only 13%, and is projected to be the second leading cause of cancer-related deaths in the United States by 2030[1,2]. Standard-of-care chemotherapy regimens have limited efficacy, in part due to a fibrotic and hypovascular tumor microenvironment (TME) that leads to poor drug delivery and uptake[3–6]. Moreover, rampant immune suppression and exclusion of cytotoxic Natural Killer (NK) and T lymphocytes in the PDAC TME,

[1]Department of Molecular, Cell, and Cancer Biology, University of Massachusetts Chan Medical School, Worcester, MA, USA. [2]Division of Hematology-Oncology, Department of Medicine, University of Massachusetts Chan Medical School, Worcester, MA, USA. [3]Department of Biomedical Engineering, University of Massachusetts Amherst, Amherst, MA, USA. [4]Cold Spring Harbor Laboratory, Cold Spring Harbor, NY, USA. [5]Department of Pathology, Zucker School of Medicine at Hofstra/Northwell, Manhasset, NY, USA. [6]Division of Innate Immunity, Department of Medicine, University of Massachusetts Chan Medical School, Worcester, MA, USA. [7]RNA Therapeutics Institute, University of Massachusetts Chan Medical School, Worcester, MA, USA. [8]Program in Molecular Medicine, University of Massachusetts Chan Medical School, Worcester, MA, USA. [9]Department of Genomics and Computational Biology, University of Massachusetts Chan Medical School, Worcester, MA, USA. [10]Cancer Center, University of Massachusetts Chan Medical School, Worcester, MA, USA. [11]Department of Radiation Oncology, University of Massachusetts Chan Medical School, Worcester, MA, USA. [12]Immunology and Microbiology Program, University of Massachusetts Chan Medical School, Worcester, MA, USA. e-mail: Marcus.Ruscetti@umassmed.edu

coupled with weak tumor immunogenicity, contribute to de novo resistance to immune checkpoint blockade (ICB) inhibitors that have demonstrated remarkable success in treating other chemo-resistant malignancies[7–9]. Hence, there is a pressing need for innovative therapeutic strategies to tackle the suppressive TME of PDAC and achieve durable tumor control.

KRAS mutations are present in >90% of PDAC lesions and drive disease onset and progression by promoting tumor cell growth and survival and remodeling the surrounding TME to mediate immune evasion[10]. We have previously shown that targeting downstream KRAS signaling with a combination of MEK inhibitor trametinib and CDK4/6 inhibitor palbociclib can promote vascularization and $CD8^+$ T cell accumulation in the TME, leading to increased sensitivity to chemotherapy and anti-PD-1 ICB[11]. These anti-tumor effects were mediated in part through induction of the senescence-associated secretory phenotype (SASP), a collection of hundreds of pleiotropic cytokines, growth and angiogenic factors, and matrix metalloproteinases that can impact the TME and in particular immune responses in dynamic ways[12]. Combining these senescence-inducing therapies with EZH2 inhibitors or STING and TLR4 agonists further enhanced the pro-inflammatory cytokine arm of the SASP, producing robust anti-tumor NK and $CD8^+$ T cell immunity that led to complete responses in preclinical PDAC mouse models[13,14]. Blockade of different SASP factors revealed key interleukins (IL-12,−15,−18), interferons (IFNβ), and chemokines (CCL2, CXCL9/10/11) necessary for anti-tumor NK and T cell immunity in PDAC following senescence induction. These findings suggest that direct delivery of SASP-related cytokines to tumors may be a novel strategy to reactivate immunity against PDAC.

Cytokines are a diverse group of small proteins that act as signaling molecules to mediate the recruitment, proliferation, and activation of various immune cells[15]. As cytokine expression is frequently altered in human cancers, cytokine administration or blockade has long been pursued as a therapeutic approach to immunologically treat tumors[16]. Dating back to the 1980/90's, systemic delivery of recombinant cytokine proteins IFNα or IL-2 that can stimulate innate and adaptive immune responses were some of the first approved immunotherapies for treating immunologically "hot" cancers like melanoma and renal cell carcinoma[17–20]. However, the modest efficacy of single cytokine administration combined with the often severe toxicities elicited by high-dose systemic delivery have limited the clinical utility of these and other cytokines such as IFNγ and IL-12[21–25]. Advances in mRNA therapeutics and drug delivery methods in recent years have offered the opportunity to revisit cytokine therapy for cancer. Indeed, work from a number of groups has shown that multiple cytokine-encoding mRNAs can be delivered intratumorally to elicit potent anti-tumor immune responses without systemic toxicities in melanoma and other "hot" tumor models[26–28].

Here, we evaluate whether multiplexed, tumor-directed administration of mRNAs encoding interleukins, interferons, and chemokines we previously demonstrated to be important for mediating innate and adaptive immunity can achieve anti-tumor immune control in "cold" and immune excluded preclinical PDAC models. We find that a combination of 5 diverse cytokine mRNAs can reactivate NK and $CD8^+$ T cell responses against PDAC tumors to reduce tumor growth and fibrosis in a safe manner. Strikingly, further integration of tumor-associated antigen (TAA) mRNAs into the cocktail could achieve potent antigen-specific $CD8^+$ T cell priming locally and systemically, leading to curative tumor responses and long-term immunity in autochthonous PDAC models. These results establish a platform for a safe and effective mRNA-based immunotherapy for advanced pancreatic cancer that currently lacks durable treatment options.

Results

Intratumoral delivery of cytokine-encoding mRNA cocktail drives safe and robust local cytokine expression in orthotopic PDAC models

We established an in vitro transcription (IVT) pipeline to synthesize mRNAs in multiplex encoding diverse cytokines we have previously demonstrated to be necessary for anti-tumor NK and T cell immunity following therapy-induced senescence in preclinical PDAC models[11,13,14], including the interleukins IL-12, IL-15, and IL-18, chemokines CCL5 and CXCL10, and the Type I interferon IFNβ (Fig. 1a). mRNAs were modified with N1-methylpseudouridine triphosphate ($m^1\Psi TP$) during IVT to enhance translational efficiency in mammalian systems and minimize activation of non-specific innate immune responses, and underwent cellulose-based purification to remove dsRNA contaminants that can produce off-target effects[29–31]. We confirmed the successful synthesis of cellulose-purified mRNA on agarose gel (Supplementary Fig. 1a). To validate their biological activity and confirm appropriate protein production and secretion, purified mRNAs were transfected into tumor cell lines derived from PDAC tumors in *Pdx1-Cre;Kras*$^{LSL\text{-}G12D/wt}$*;Trp53*$^{LSL\text{-}R172H/wt}$ (*KPC*) genetically engineered mouse models (GEMMs), as well as cancer-associated fibroblast (CAF) lines derived from PDAC tumors in *Pdx1-Cre;* *Kras*$^{LSL\text{-}G12D/wt}$*;Trp53*$^{LSL\text{-}R172H/wt}$;Rosa26$^{LSL\text{-}YFP/LSL\text{-}YFP}$ (*KPCY*) GEMMs[32,33]. Lipofectamine transfection of 6 cytokine mRNAs (*Il12, Il15, Il18, Ccl5, Cxcl10, Ifnb*) simultaneously in vitro yielded a significant and robust increase in secreted amounts of all cytokines 24 h post-transfection in tumor cells and to an even greater degree in CAFs that are highly prevalent in the desmoplastic PDAC TME (Supplementary Fig. 1b, c). The level of secretion of many of these cytokines after mRNA transfection was an order of magnitude higher compared to their quantities following treatment of tumor cells with trametinib and palbociclib (T/P), which we have previously[11] and now here demonstrated could induce their expression as part of an NF-κB-driven SASP following senescence induction (Supplementary Fig. 1d–g). This highlights the potential of this mRNA approach to produce a pro-inflammatory cytokine milieu in the PDAC TME.

We next evaluated the capacity of these mRNAs to produce secreted cytokines within PDAC tumors in C57BL/6 mice orthotopically transplanted with *KPC1* tumor cells. Once tumors in the pancreas were confirmed by ultrasound imaging (10-12 days post-surgery), the cocktail of 6 free (naked) cytokine-encoding mRNAs (*Il12, Il15, Il18, Ccl5, Cxcl10, Ifnb*) at 10 μg per mRNA, or 60 μg of scrambled mRNA as a control, was administered intratumorally (Fig. 1b). Cytokine array analysis demonstrated increased quantities of each of the cytokines encoded by their corresponding mRNAs within the tumor milieu 24 h post-injection (Fig. 1c). 10 μg of free *Il12* mRNA produced a similar induction of IL-12 protein levels as either 60 μg of free *Il12* mRNA or 10 μg of lipid nanoparticle (NP) encapsulated *Il12* mRNA delivered intratumorally (Supplementary Fig. 1h, i), demonstrating that the low doses of free mRNA we are using are sufficient for cytokine protein production in vivo. This pulse in cytokine induction was transient, as their expression was reduced after 48 h and returned to baseline for most cytokines 96 h after mRNA dosing (Fig. 1c). With the exception of chemokines CCL5 and CXCL10 that act through gradients to promote immune chemotaxis, levels of other cytokines did not change significantly in the blood or systemically in the liver after intratumoral cytokine mRNA administration (Fig. 1d and Supplementary Fig. 1j). Importantly, treatment was well-tolerated, with no significant changes in body weight observed in mice treated with cytokine mRNAs as compared to control Scramble mRNAs (Fig. 1e).

Broader cytokine array analysis at 96 h post-injection revealed altered levels of other cytokines not delivered in the mRNA cocktail (Supplementary Fig. 1k). In particular, we observed a significant

https://doi.org/10.1038/s41467-026-74574-z

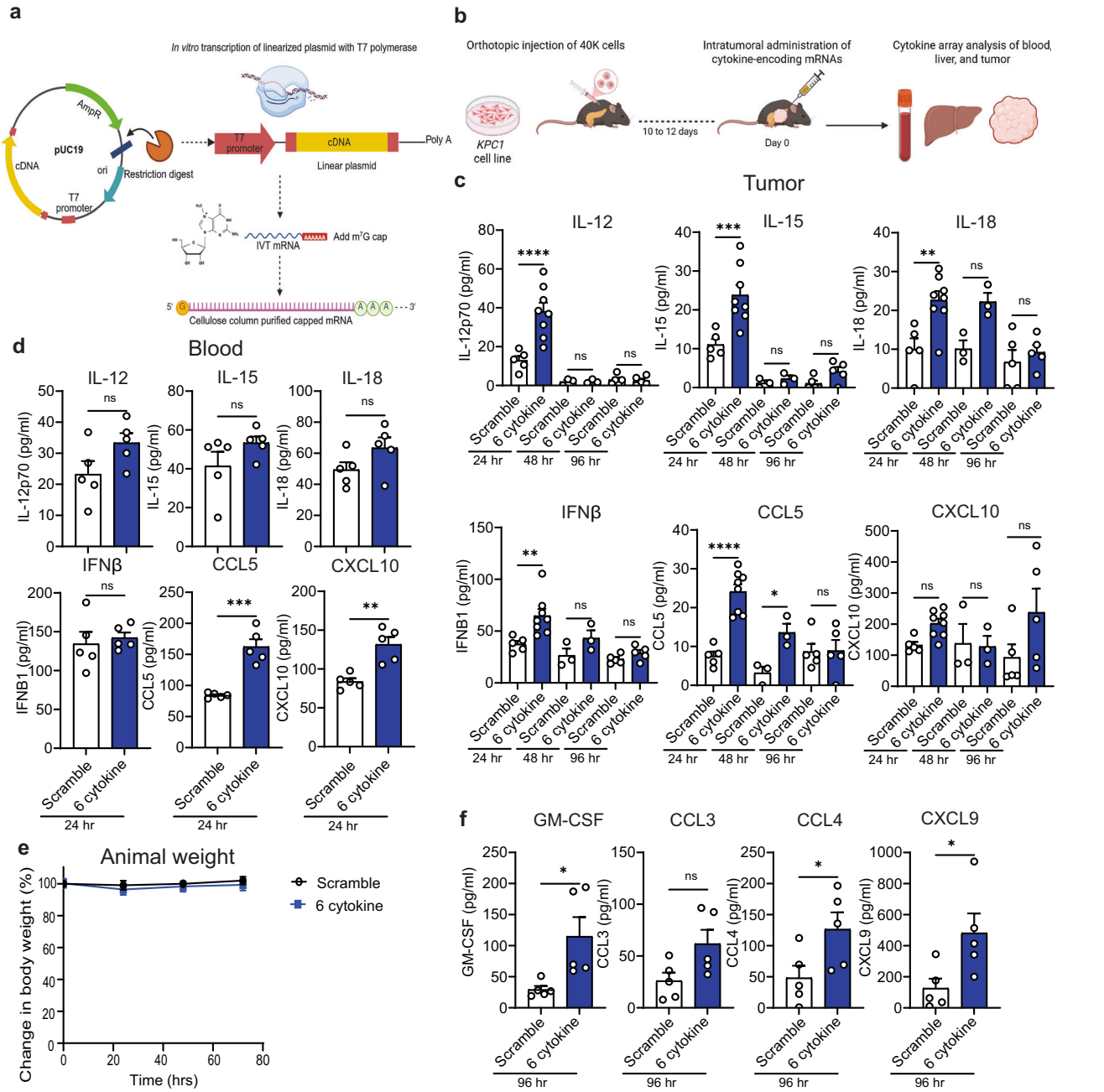

Fig. 1 | Cytokine mRNA administration drives safe and robust local cytokine expression following intratumoral injection into orthotopic PDAC models. **a** Schematic of mRNA synthesis pipeline. Created in BioRender. Ma, B. (2026) https://BioRender.com/whgkbpu. **b** *KPC1* PDAC tumor cells expressing luciferase-GFP were orthotopically injected into the pancreas of 8- to 12-week-old female C57BL/6 mice. Following tumor establishment, mice received intratumoral injections of 60 μg of either scramble mRNA or a 6-cytokine mRNA cocktail (10 μg each of IL-12, IL-15, IL-18, IFNβ, CCL5, and CXCL10). Tumor, liver, and blood samples were collected at 24-, 48-, and 96-hours (h) post-injection for cytokine array analysis. Created in BioRender. Ma, B. (2026) https://BioRender.com/hml8h8o. Cytokine array results from tumor tissues (**c**) (Scramble (24 h), $n = 5$; 6 Cytokine (24 h), $n = 8$; Scramble (48 h), $n = 3$; 6 Cytokine (48 h), $n = 3$; Scramble (96 h), $n = 5$; 6 Cytokine (96 h), $n = 5$ mice) and blood (**d**) ($n = 5$ mice per group) collected at indicated time points following intratumoral mRNA administration as described in **b**. Cytokine array results from tumors represent a pool of two independent experiments. **e** Change in weight of *KPC1* tumor-bearing mice at 24-, 48-, and 72 h following one intratumoral dose of either scramble mRNA (60 μg) or a 6-cytokine mRNA cocktail (10 μg each of IL-12, IL-15, IL-18, IFNβ, CCL5, and CXCL10; 60 μg total) ($n = 5$ mice per group). **f** Cytokine array results from tumor tissues collected at 96 h post-intratumoral mRNA administration as described in **b** ($n = 5$ mice per group). *P* values in **c** were calculated using ordinary one-way ANOVA with Sidák's correction, and those in **d**, **f** using two-tailed, unpaired Student's *t*-test. Data are presented as mean ± s.e.m. ns, not significant; $^{*}P < 0.05$; $^{**}P < 0.01$; $^{***}P < 0.001$; $^{****}P < 0.0001$. Source data are provided as a Source data file.

increase in expression of GM-CSF, a key cytokine involved in dendritic cell (DC) differentiation and pro-inflammatory responses[34,35], as well as chemokines CCL3, CCL4, and CXCL9 that are important drivers of NK and T cell recruitment and associated with better anti-PD-1 immunotherapy responses[36–38] (Fig. 1f). On the other hand, other pro-inflammatory cytokines known to be induced by endogenous mRNAs through activating Toll-like receptors (IL-1α, IL-1β, IL-6, TNF)[31,39] were not significantly altered following injection of our cytokine mRNAs engineered with synthetic nucleoside modifications (Supplementary Fig. 1k). Together, these findings demonstrate that intratumoral administration of a low dose cytokine-encoding mRNA cocktail not only safely augments local expression of the delivered cytokines, but

also induces a secondary wave of cytokines that could potentially amplify anti-tumor immune responses.

mRNA multiplexing uncovers optimal cytokines to enhance tumor immunogenicity and activate NK and CD8$^+$ T cell responses in PDAC ex vivo

Given the modularity of our mRNA synthesis pipeline, we set out to investigate the contribution of individual cytokines to different arms of the immune response to determine the optimal combination to mediate effective anti-tumor immunity in PDAC. One of the first hurdles to anti-tumor immunity is the inability of cytotoxic lymphocytes such as NK and CD8$^+$ T cells to infiltrate into the PDAC TME. As such, we first performed in vitro transwell migration assays with NK or CD8$^+$ T cells purified from mouse spleens in the top chamber and conditioned media from *KPC* PDAC tumor cells transfected with different single or combinatorial mRNA formulations in the bottom chamber to assess the impact of cytokines on lymphocyte chemotaxis (Supplementary Fig. 2a). While individual cytokine mRNAs tested (IL-12, IL-18, CCL5, CXCL10) were not sufficient on their own to promote NK cell chemotaxis, the combination of all six together significantly increased NK cell migration in vitro compared to control Scramble mRNA (Supplementary Fig. 2b). IL-18 and CCL5 were necessary for NK cell chemotaxis, as their omission from the 6 cytokine mRNA cocktail reversed its NK cell migratory effects. On the other hand, IL-15 was dispensable, with the resulting 5 cytokine combination (IL-12, IL-18, CCL5, CXCL10, IFNβ) sufficient to promote NK cell migration (Supplementary Fig. 2b). Similarly, a combination of 4 mRNAs encoding cytokines IL-12, IL-18, IFNβ, and CXCL10 produced significantly increased CD8$^+$ T cell migration through a transwell insert, with again IL-15 and now CCL5 being unnecessary (Supplementary Fig. 2c).

We next co-cultured murine NK or CD8$^+$ T cells with mRNA-transfected *KPC* PDAC tumor cells and assessed the impact on lymphocyte effector functions as measured by IFNγ production (Supplementary Fig. 2d). Flow cytometry analysis of NK cells revealed that the combination of all 6 cytokines, or 5 cytokines without IL-15, was required for IFNγ induction (Supplementary Fig. 2e, g), with again IL-18 and CCL5 being necessary, matching the cytokine requirements we uncovered for NK cell migration in vitro. For CD8$^+$ T cells, the combination of 4 mRNAs encoding cytokines IL-12, IL-18, IFNβ, and CXCL10 was sufficient to significantly increase CD8$^+$ T cell IFNγ production (Supplementary Fig. 2f, g). Collectively, these results demonstrate that multiple mRNA cytokines are needed to promote NK and T cell chemotaxis and effector functions, and that IL-15 is dispensable for these phenotypes.

Antigen-dependent CD8$^+$ effector T cell responses rely on the recognition of antigens expressed on the surface of tumor cells through major histocompatibility complex class I (MHC-I) molecules, which are generally lowly expressed in PDAC[40,41]. To investigate if cytokine mRNAs could also enhance pancreatic tumor cell immunogenicity through upregulating MHC-I, *KPC* cells were transfected with individual mRNAs encoding IL-12 and IFNβ that have established roles[42,43] in inducing MHC-I alone or as part of the full six cytokine mRNA cocktail. MHC-I surface expression was assessed by flow cytometry analysis 24 h post-transfection. Whereas IL-12 mRNAs had no impact on MHC-I levels, IFNβ mRNA significantly enhanced MHC-I expression on tumor cells (Supplementary Fig. 2h). The full 6 cytokine mRNA combination significantly increased MHC-I intensity compared to IFNβ mRNA treatment alone, demonstrating that use of cytokine combinations can further enhance antigen presentation. Still, mRNA combinations lacking IFNβ (3 cytokine and 5 cytokine groups), as well as co-administration of the 6 cytokine mRNAs with an antibody neutralizing the Type I interferon receptor (IFNAR), failed to induce MHC-I upregulation, underscoring the essential role of IFNβ in driving tumor antigen presentation (Supplementary Fig. 2h, i). Collectively, these findings provided strong rationale for the delivery of a combination of mRNAs encoding ILs, IFNs, and chemokines to fully elicit NK and CD8$^+$ T cell migration and activation and antigen presentation required to achieve anti-tumor immunity against PDAC.

Intratumoral administration of cytokine mRNA cocktail activates innate and adaptive immunity and produces anti-tumor and fibrotic effects in PDAC-bearing mice

We next aimed to determine if cytokine mRNAs could alter immune responses in the PDAC TME in vivo in mice bearing orthotopically transplanted *KPC1* tumors that we have previously shown to be immunologically "cold"[11,13,14]. Given the transient nature of cytokine expression following intratumoral mRNA administration (Fig. 1c), we conducted repeated intratumoral injections of our cytokine mRNA cocktail every three days to enable long-term assessment of the immune response over a 12-day period (Fig. 2a). In addition to some mice receiving combinations of 10 µg each of IL-12, IL-18, IFNβ, CXCL10, and CCL5 mRNAs with (6 cytokine cocktail) or without (5 cytokine cocktail) IL-15 mRNA that we showed to be dispensable in vitro, other cohorts were injected intratumorally with 10 µg of each single cytokine mRNA alone for comparison.

Flow cytometry analysis performed after four intratumoral injections revealed that individual cytokine mRNAs within the cocktails could produce non-overlapping innate and adaptive immune effects in the "cold" PDAC TME. While no cytokine mRNAs were capable of increasing T cell numbers in "cold" *KPC1* PDAC tumors, IL-12 mRNAs alone, which other recent reports have shown to activate anti-tumor T cell immunity in PDAC mouse models[44,45], were indeed able to increase effector CD8$^+$ T cell differentiation and induce their expression of IFNγ in *KPC1* PDAC tumors compared to Scramble mRNAs (Supplementary Fig. 3a–d). Still, in our model, IL-12 mRNA alone was not sufficient to activate innate DC and NK cell responses or remodel suppressive myeloid cell populations (Fig. 2b–e and Supplementary Fig. 3e–i). IL-18, CCL5, and IFNβ, on the other hand, each contributed profoundly to immune remodeling in diverse ways. Single IL-18 mRNA dosing significantly increased the proportion of both effector and memory CD8$^+$ T cells to a greater extent than IL-12 mRNA, as well as was sufficient to induce IFNγ/GZMB co-expression in polyfunctional CD4$^+$ T cells (Fig. 2f, g and Supplementary Fig. 3j, k). The chemokine CCL5 was capable of activating IFNγ production in NK cells when delivered as a single mRNA (Fig. 2e). Alternatively, IFNβ mRNA alone directed the infiltration of cross-presenting CD103a$^+$ DCs that are essential for T cell priming in tumors (Fig. 2b).

Though each cytokine alone could contribute to eliciting a different immune phenotype, when delivered together, the 5-cytokine (5C) and 6-cytokine (6C) mRNA combinations were able to activate cytotoxic NK and CD8$^+$ T cell responses in a manner that could not be achieved with any single cytokine mRNA. Combinatorial, but not individual, cytokine mRNA administration led to enhanced NK cell accumulation and cytotoxicity as marked by expression of cytolytic Granzyme B (GZMB)$^+$ granules (Fig. 2c, d and Supplementary Fig. 3f, g). Remarkably, only the 5C combination could activate polyfunctional CD8$^+$ T cells marked by co-expression of IFNγ and GZMB (Fig. 2h). Additionally, whereas MHC-II$^+$ F4/80$^+$ macrophage numbers were largely unchanged across treatment groups, the 5C cocktail led to a trend toward a reduction in CD206$^+$ 'M2'-like macrophages known to have immune suppressive characteristics (Supplementary Fig. 3l,m). Interestingly, whereas the 6C mRNA combination containing IL-15 led to significant mobilization of Gr-1$^+$ myeloid-derived suppressor cells (MDSCs) that can mediate NK and T cell suppression in the TME, the 5C cocktail lacking IL-15 had no impact on MDSC numbers (Supplementary Fig 3h, i). The 5C mRNA combination is thus able to effectively activate innate and adaptive immune responses while simultaneously remodeling the immune suppressive "cold" TME of PDAC.

Treatment with the 5 and 6 cytokine mRNA cocktails also had a marked impact on PDAC tumors and their surrounding stroma. Myofibroblasts prevalent within PDAC lesions contribute to a desmoplastic TME that can restrict the infiltration of NK and T cells[46].

https://doi.org/10.1038/s41467-026-74574-z

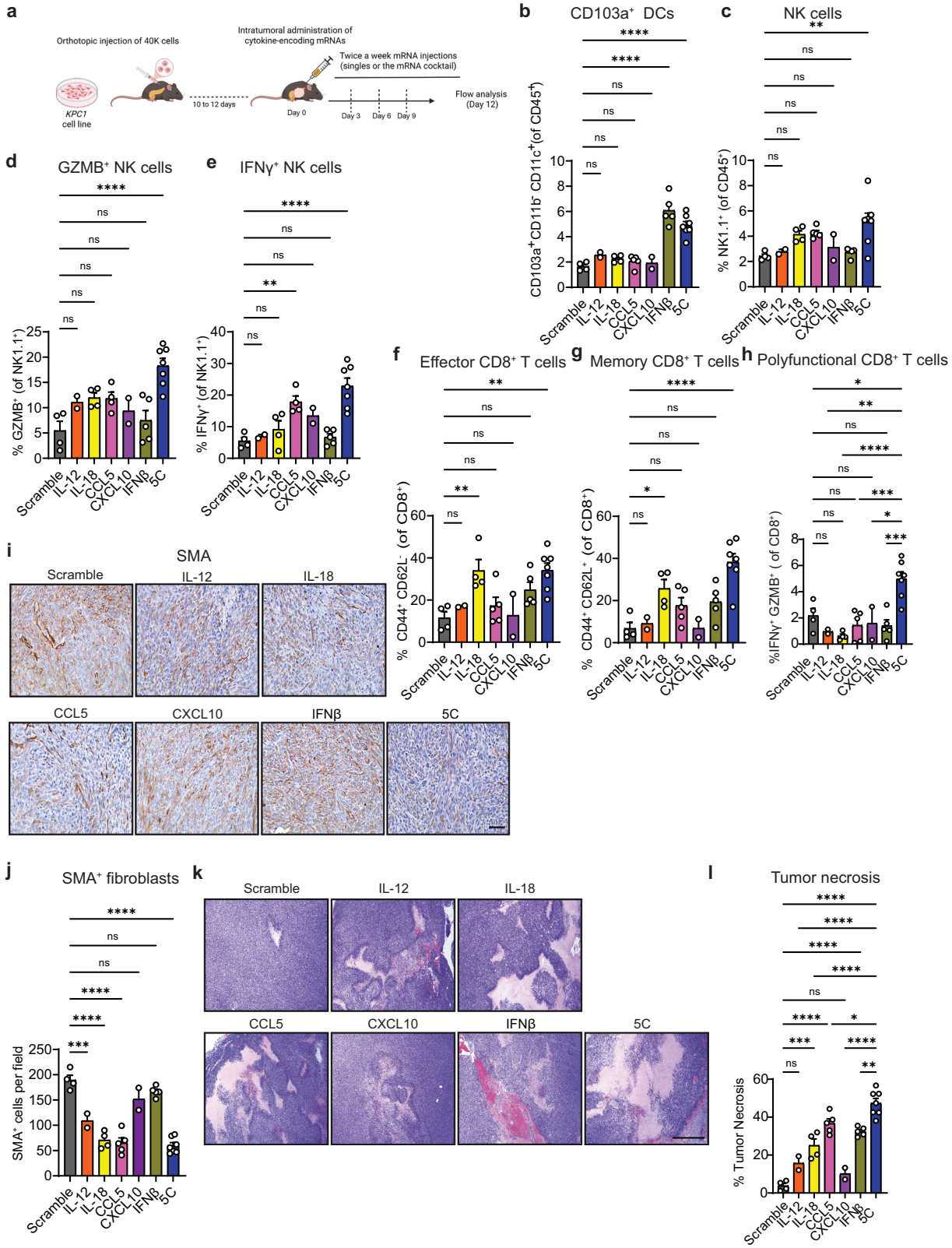

Immunohistochemical (IHC) staining analysis revealed a significant reduction in smooth muscle actin (SMA)$^+$ and PDGFRβ$^+$ myofibroblasts, as well as FAP$^+$ activated cancer-associated fibroblasts (CAFs) in PDAC tumors following 12 day treatment with the multiplexed cytokine mRNA combinations (Fig. 2i, j and Supplementary Fig. 4a–f). In addition, trichrome staining further revealed that 5C mRNA administration could dramatically reduce collagen levels in the desmoplastic stroma of the PDAC TME (Supplementary Fig. 4g, h). Interestingly, this reduction in fibroblasts and collagen was mediated primarily through IL-18 and CCL5 mRNAs (Fig. 2i, j and Supplementary Fig. 4c–h). Changes in tumor growth and necrosis were also assessed after 12-day treatment. Both the 5 and 6 cytokine combinations, and even IFNβ mRNAs alone, could significantly reduce tumor growth compared to Scramble mRNA controls (Supplementary Fig. 4i, j). However, while IL-

Fig. 2 | A multiplexed cytokine mRNA cocktail mobilizes innate and adaptive immunity and reduces tumor growth and desmoplasia in "cold" PDAC-bearing mice. a *KPC1* PDAC tumor cells expressing luciferase-GFP were orthotopically injected into the pancreas of 8- to 12-week-old female C57BL/6 mice. Following tumor establishment, mice received intratumoral injections of either Scramble (50 μg), IL-12 (10 μg), IL-18 (10 μg), IFNβ (10 μg), CCL5 (10 μg), or CXCL10 mRNAs (10 μg), or a 5-cytokine mRNA cocktail (10 μg each of IL-12, IL-18, IFNβ, CCL5, and CXCL10; 50 μg total). Injections were administered every 3 days, and mice were euthanized for downstream tumor analysis on Day 12. Created in BioRender. Ma, B. (2026) https://BioRender.com/owmho90. Flow cytometry analysis of percentages of CD103a$^+$ cross-presenting dendritic cells (DCs) (**b**), total NK1.1$^+$ NK cells (**c**), GZMB$^+$ NK cells (**d**), IFNγ$^+$ NK cells (**e**), effector CD44$^+$CD62L$^-$ CD8$^+$ T cells (**f**), memory CD44$^+$CD62L$^+$ CD8$^+$ T cells (**g**), and polyfunctional IFNγ$^+$GZMB$^+$ CD8$^+$ T cells (**h**) in *KPC1* orthotopic PDAC tumors following repeated mRNA treatment as in **a** (Scramble, $n = 4$; IL-12, $n = 2$; IL-18, $n = 4$; CCL5, $n = 4$ or 5; CXCL10, $n = 2$; IFNβ, $n = 5$; 5C, $n = 7$ mice). **i** Representative immunohistochemical (IHC) staining of *KPC1* orthotopic PDAC tumors from mice treated for 12 days as in **a**. Scale bar, 100 μm. **j** Quantification of SMA$^+$ myofibroblasts per field from IHC analysis in **i** (Scramble, $n = 4$; IL-12, $n = 2$; IL-18, $n = 4$; CCL5, $n = 5$; CXCL10, $n = 2$; IFNβ, $n = 5$; 5C, $n = 7$ mice). **k** H&E staining of *KPC1* orthotopic PDAC tumors following 12 day treatment of mice as in **a**. Scale bar, 500 μm. **l** Quantification of the percentage of tumor area covered in necrosis (Scramble, $n = 4$; IL-12, $n = 2$; IL-18, $n = 4$; CCL5, $n = 5$; CXCL10, $n = 2$; IFNβ, $n = 5$; 5C, $n = 7$ mice). *P* values in **b**–**g**, **j** were calculated using ordinary one-way ANOVA with Dunnett's correction, and those in **h**, **l** were calculated using ordinary one-way ANOVA with Tukey's correction. Data are presented as mean ± s.e.m. ns, not significant; $^*P < 0.05$; $^{**}P < 0.01$; $^{***}P < 0.001$; $^{****}P < 0.0001$. Source data are provided as a Source data file.

18, CCL5, and IFNβ mRNA administration alone could induce tumor necrosis compared to control Scramble mRNAs, the 5C combination significantly enhanced tumor necrosis compared to any single cytokine mRNA alone, aligned with the ability of the cytokine cocktail to mediate cytotoxic lymphocyte activity (Fig. 2k–l). Consistent with this cell death phenotype, we also observed an increase in cleaved caspase-3 positive apoptotic cells, but no change in cellular proliferation as marked by Ki67, following multiplexed cytokine mRNA treatment (Supplementary Fig. 4k). In contrast, these cytokine mRNAs had minimal impact on *KPC* tumor cell and CAF viability in vitro, suggesting that the anti-tumor and fibrotic effects observed in vivo are unlikely the result of the direct effects of cytokine production on tumor cells and fibroblasts (Supplementary Fig. 4l, m). Together, these results demonstrate that multiplexed cytokine mRNA therapy combines effectively to activate NK and CD8$^+$ T cell effector functions, alleviate fibrosis, and produce anti-tumor responses in PDAC.

Combinatorial cytokine mRNA therapy can achieve robust cytotoxic T cell responses in a "hot" PDAC model expressing neo-antigens

The *KPC1* orthotopic PDAC model is immunologically "cold" and lacks neo-antigens necessary for robust cytotoxic T cell responses[11]. To test our cytokine mRNA cocktail in a "hot" PDAC model, we orthotopically implanted the syngeneic *KPCY 2838c3* cell line, which was previously shown to exhibit a T cell-high phenotype and contain three predicted neoantigens[47], into C57BL/6 mice. Indeed, we confirmed that transplanted *KPCY 2838c3* tumors have increased numbers of total CD3$^+$ and CD8$^+$ T cells, as well as higher expression of IFNγ associated with a "hot" TME, compared to *KPC1* tumors (Supplementary Fig. 5a, b). Given our in vitro and in vivo findings that IL-15 mRNAs included in the 6C mRNA combination are not necessary for inducing NK and CD8$^+$ T cell migration and effector functions (see Fig. 2c–h and Supplementary Fig. 2a–f), we moved forward with the 5C mRNA cocktail (IL-12, IL-18, CCL5, CXCL10, IFNβ) excluding IL-15 for subsequent studies.

Following *KPCY 2838c3* tumor formation (as assessed by ultrasound), control Scramble mRNA, the 5 cytokine mRNA combination, or IL-12 mRNA alone for comparison, was injected intratumorally twice per week (Fig. 3a). Flow cytometry analysis after 12 day treatment showed an increase in total CD45$^+$ immune cell infiltration accompanied by a significant expansion of both total as well as CD8$^+$ and CD4$^+$ T cell subsets in the 5C mRNA cocktail but not single IL-12 mRNA group (Fig. 3b and Supplementary Fig. 5c, d). Though both IL-12 alone and combined 5C mRNAs enhanced the percentage of effector and memory CD8$^+$ T cells in the PDAC TME compared to control Scramble mRNA, a significant increase in polyfunctional cytotoxic CD8$^+$ T cells (IFNγ$^+$GZMB$^+$) was only observed in the 5C mRNA arm (Fig. 3c, d). CD4$^+$ T cell effector functions were unaltered by cytokine mRNA administration in this model (Supplementary Fig. 5e). Despite no change in total NK cell numbers in this T cell-high *KPCY* PDAC model, there was a significant increase in their expression of effector cytokine IFNγ and cytotoxic GZMB granules following cytokine therapy (Fig. 3e and Supplementary Fig. 5f). There was also a significant increase in CD103a$^+$ cross-presenting DCs and MHC-II$^+$ macrophages, as well as a decrease in MDSCs in both IL-12 and combinatorial 5-cytokine mRNA conditions that could further support T cell priming and activity in the PDAC TME (Fig. 3f and Supplementary Fig. 5g). Ultrasound imaging of PDAC tumors revealed that while repeated IL-12 mRNA dosing alone did not alter tumor growth, treatment with the 5 cytokine mRNA cocktail led to significant tumor growth reduction after 12 day treatment compared to Scramble mRNA (Fig. 3g). Thus, despite the capacity of IL-12 mRNA alone to increase the percentages of cross-presenting DCs, effector and memory CD8$^+$ T cells, and activated NK cells in an immunologically "hot" PDAC transplant model, only the 5 cytokine combination was able to elicit robust CD8$^+$ T cell infiltration and polyfunctional activation necessary for tumor growth suppression.

Given the anti-tumor immune responses produced by repeated cytokine mRNA administration, we were curious if a single injection of the 5C mRNA cocktail could achieve similar outcomes in the *KPCY 2838c3* PDAC transplant model (Fig. 3h). Flow cytometry analysis performed 72 h post-treatment with a single mRNA dose revealed a significant increase in overall CD45$^+$ immune cell infiltration, along with expansion of total and CD8$^+$ T cell numbers, effector and memory CD8$^+$ T cell populations, NK cell effector functions, and MHC-II$^+$ macrophages in tumors treated with the 5C mRNA cocktail compared to Scramble control mRNAs (Fig. 3i-m and Supplementary Fig. 5h), similar to what was observed in tumors following multi-dosing over 12 days. Although total NK and CD4$^+$ T cell numbers remained unchanged as with long-term treatment, short-term 5C mRNA therapy significantly increased the frequency of polyfunctional IFNγ$^+$GZMB$^+$ CD4$^+$ T cells not observed following 12-day treatment, indicating an early activation of CD4$^+$ T cell effector functions with cytokine mRNAs (Supplementary Fig. 5i–k). In contrast, MDSC numbers that were reduced after repeated 12-day treatment remained unaffected 3 days after a single cytokine mRNA injection (Supplementary Fig. 5l). Moreover, while there was a trend toward increased cross-presenting DCs and polyfunctional CD8$^+$ T cells 3 days after mRNA injection of the 5C cocktail, these changes were not significant compared to 12-day repeated dosing, suggesting that remodeling of the myeloid compartment and full CD8$^+$ T cell priming may occur over longer periods (Fig. 3n, o). Still, 2 weeks after a single intratumoral mRNA injection, ultrasound imaging revealed significant tumor growth control in the 5C mRNA group compared to the cohort receiving control Scramble mRNA (Fig. 3p). Even more strikingly, a single dose of the 5 cytokine mRNAs was able to significantly increase overall survival in mice bearing *KPCY 2838c3* PDAC tumors (Fig. 3q). We further compared single dose administration of the 5C mRNA cocktail at 10 μg versus 60 μg per mRNA in *KPCY 2838c3* transplant tumors to define a tolerable and efficacious dose range. While both doses were sufficient to reduce tumor growth over 72 h compared with Scramble mRNA controls, the 60 μg dose led to a trend towards increased serum ALT levels, indicative of

https://doi.org/10.1038/s41467-026-74574-z

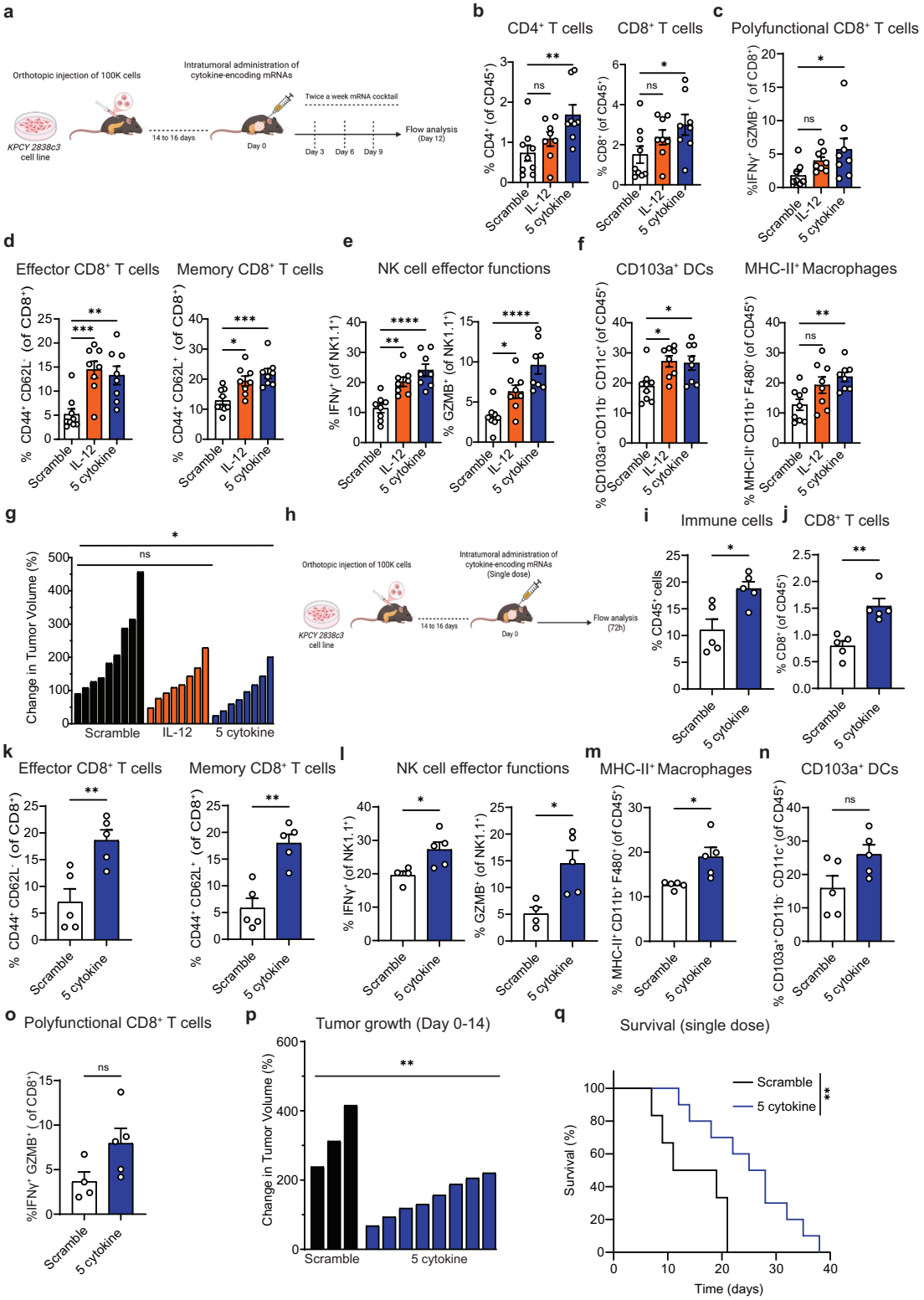

hepatotoxicity, and caused significant body weight loss, whereas the 10 μg dose was well-tolerated (Supplementary Fig. 5m–o). Collectively, these results demonstrate that anti-tumor immune responses can be produced in an immunologically "hot" PDAC model in a safe manner after a single low dose of cytokine mRNAs, and suggest that the presence of tumor antigens may further enhance the robustness of T cell responses to cytokine therapies to sustain immunity against PDAC.

Co-delivery of cytokine- and antigen-encoding mRNAs enhances antigen-presentation and T cell anti-tumor immunity in a "cold" PDAC model

Our above findings highlight the synergistic potential of combining cytokine-encoding mRNAs with strategies to enhance tumor-specific T cell priming in PDAC. Recent clinical trials have explored neo-antigen-encoding mRNA vaccines as a therapeutic strategy for PDAC,

Fig. 3 | Combinatorial cytokine mRNA therapy can achieve robust cytotoxic T cell immunity in a "hot" PDAC model after a single dose. a *KPCY 2838c3* PDAC tumor cells were orthotopically injected into the pancreas of 8- to 12-week-old female C57BL/6 mice. Following tumor establishment, mice received intratumoral injections of either Scramble (50 μg) or IL-12 mRNAs (10 μg), or a 5-cytokine mRNA cocktail (10 μg each of IL-12, IL-18, IFNβ, CCL5, and CXCL10; 50 μg total). Injections were administered every 3 days, and mice were euthanized for downstream tumor analysis on Day 12. Created in BioRender. Ma, B. (2026) https://BioRender.com/sls6ii2. Flow cytometry analysis of total $CD8^+$ and $CD4^+$ T cells (**b**) (Scramble, $n = 9$; IL-12, $n = 8$; 5 cytokine, $n = 8$ mice), polyfunctional $IFN\gamma^+GZMB^+$ $CD8^+$ T cells (**c**) (Scramble, $n = 8$; IL-12, $n = 8$; 5 cytokine, $n = 8$ mice), effector and memory $CD8^+$ T cells (**d**) (Scramble, $n = 9$; IL-12, $n = 8$; 5 cytokine, $n = 8$ mice), NK cell effector functions (**e**) (Scramble, $n = 8$; IL-12, $n = 8$; 5 cytokine, $n = 8$ mice), and antigen-presenting $CD103a^+$ DCs and MHC-II^+ macrophages (**f**) (Scramble, $n = 9$; IL-12, $n = 8$; 5 cytokine, $n = 8$ mice) in *KPCY 2838c3* orthotopic PDAC tumors following indicated mRNA treatment as in **a**. **g** Waterfall plot of the response of *KPCY 2838c3* orthotopic PDAC tumors to 12-day treatment as in **a** (Scramble, $n = 9$; IL-12, $n = 8$; 5 cytokine, $n = 8$ mice). **h** *KPCY 2838c3* PDAC tumor cells were orthotopically injected into the pancreas of 8- to 12-week-old female C57BL/6 mice. Following tumor establishment, mice received a single intratumoral injection of either Scramble mRNA (50 μg) or a 5-cytokine mRNA cocktail (10 μg each of IL-12, IL-18, IFNβ, CCL5, and CXCL10; 50 μg total). Created in BioRender. Ma, B. (2026) https://BioRender.com/xnv17n4. Flow cytometry analysis of total $CD45^+$ immune cells (**i**) ($n = 5$ mice per group), total $CD8^+$ T cell populations (**j**) ($n = 5$ mice per group), effector and memory $CD8^+$ T cells (**k**) ($n = 5$ mice per group), NK cell effector functions (**l**) (Scramble, $n = 4$; 5 cytokine, $n = 5$ mice), MHC-II^+ macrophages (**m**) ($n = 5$ mice per group), $CD103a^+$ cross-presenting DCs (**n**) ($n = 5$ mice per group), and polyfunctional $IFN\gamma^+$ $GZMB^+$ $CD8^+$ T cells (**o**) (Scramble, $n = 4$; 5 cytokine, $n = 5$ mice) in *KPCY 2838c3* orthotopic PDAC tumors 72 h following indicated mRNA treatment as in **h**. **p** Waterfall plot of the response of *KPCY 2838c3* orthotopic PDAC tumors to 14-day treatment as in **h** (Scramble, $n = 3$; 5 cytokine, $n = 8$ mice). **q** Kaplan–Meier survival curve of mice with *KPCY 2838c3* orthotopic PDAC tumors treated with a single intratumoral injection of mRNAs as in **h** (Scramble, $n = 6$; 5 cytokine, $n = 10$ mice). *P* values in **b**–**g** were calculated using ordinary one-way ANOVA with Dunnett's correction, and those in **i**–**p** using two-tailed, unpaired Student's *t*-test. *P* values in **q** were calculated using a log-rank test. Data are presented as mean ± s.e.m. ns, not significant; $^*P < 0.05$; $^{**}P < 0.01$; $^{***}P < 0.001$; $^{****}P < 0.0001$. Source data are provided as a Source data file.

demonstrating improved patient survival through the induction of long-lasting tumor antigen-specific T cell immunity following tumor resection[48,49]. Hence, we hypothesized that integrating mRNAs encoding tumor-associated antigens (TAAs) into our existing cytokine mRNA cocktail as an all-in-one therapy approach could further enhance and prolong anti-tumor T cell responses, particularly in the setting of a "cold" PDAC TME.

To this end, we generated mRNAs encoding three well-characterized PDAC TAAs—Mesothelin (MSLN)[50], Mucin-1 (MUC-1)[51], and Prostate-Specific Membrane Antigen (PSMA)[52]. Upon intratumoral delivery of these 3 antigen-encoding mRNAs as a cocktail into the *KPC1* PDAC tumor model, MSLN, MUC-1, and PSMA protein surface expression were measurably increased in tumors 24 h post-injection as compared to control Scramble mRNA injection as assessed by IHC analysis (Fig. 4a, b). To determine if intratumoral delivery of these TAA mRNAs could effectively generate antigen-specific T cells within the PDAC TME, we devised an ex vivo antigen stimulation assay. Splenocytes were first isolated from naïve C57BL/6 mice and pulsed with antigen-encoding mRNAs for 24 h ex vivo. In parallel, T cells were isolated from tumors of PDAC-bearing mice that had been vaccinated intratumorally with the same antigen-encoding mRNAs 72 h prior (Supplementary Fig. 6a). Antigen-specific activation of $CD8^+$ T cells from tumor-bearing mice vaccinated with the 3-antigen mRNA cocktail was confirmed by a marked increase in $IFN\gamma^+$ $GZMB^+$ polyfunctional $CD8^+$ T cells following exposure to antigen-mRNA-pulsed splenocytes (Supplementary Fig. 6b).

Having validated the capacity of the 3-antigen mRNA combination to generate antigen-specific T cells in PDAC tumors, we set out to investigate the impact of these engineered TAA mRNAs alone or as part of an all-in-one cocktail with the 5 cytokine-encoding mRNA combination on immune responses in the "cold" *KPC1* PDAC mouse model (Fig. 4a). Repeated intratumoral administration of the 3 antigen-encoding mRNA (3A) cocktail on its own over 12 days had little impact on innate and adaptive immune responses outside of increasing $CD103a^+$ DC frequencies (Fig. 4c–e and Supplementary Fig. 6c–j). While both the 5-cytokine (5C) mRNA cocktail alone or in combination with antigen mRNAs (5C + 3A) could achieve a similar increase in NK cell numbers and activation and expansion in effector and memory $CD8^+$ T cell populations, only the 5C + 3A all-in-one mRNA combination, but not 5C or 3A alone, induced a significant increase in numbers of polyfunctional $IFN\gamma^+GZMB^+$ polyfunctional $CD8^+$ as well as $CD4^+$ T cells compared to Scramble mRNAs (Fig. 4d and Supplementary Fig. 6f–i). Moreover, co-injection of cytokine and antigen mRNAs together significantly enhanced the numbers of cross-presenting $CD103a^+$ DCs, as well as shifted the macrophage population from a $CD206^+$ M2 phenotype toward an antigen-presenting MHC-II^+ M1 phenotype compared to cytokine or antigen mRNA regimens alone (Fig. 4c, e). MDSC numbers, on the other hand, remained unchanged across conditions (Supplementary Fig. 6j). Thus, the addition of TAAs to the 5 cytokine mRNA package is able to further enhance antigen-presentation and effector functionality of $CD4^+$ and $CD8^+$ T cells.

PDAC tumors from 5C + 3A mRNA treated mice also displayed extensive tumor necrosis, as visible by gross histology, that was further heightened compared to 5-cytokine or 3-antigen mRNA administration alone (Fig. 4f, g). Ultrasound analysis demonstrated that dosing with the combination of 3 antigen and 5 cytokine-encoding mRNAs translated into significant tumor growth suppression in *KPC1* PDAC transplant mice (Fig. 4h). Together, these results demonstrate that cytokine and antigen mRNA therapy modalities synergize to prime T cell activity in the "cold" PDAC TME and produce anti-tumor immune responses.

Combined cytokine- and antigen-encoding mRNA administration enhances T cell priming and activation through DC antigen-presentation in tumor-draining lymph nodes

Tumor-draining lymph nodes (tdLNs) are important hubs for antigen presentation and T cell priming that are necessary for sustained anti-tumor immune responses and immunotherapy efficacy[53]. In order to assess the impact of cytokine and antigen mRNA therapy on systemic immune responses in the tdLNs, we transplanted *KPC1* PDAC tumor cells into C57BL/6 mice subcutaneously, which enables efficient recovery and characterization of the corresponding lymph nodes. Following subcutaneous PDAC tumor development, mice received repeated intratumoral dosing of Scramble, 5-cytokine, or 3-antigen mRNAs alone or together every 3 days over the course of 12 days (Fig. 5a).

The tdLNs after repeated intratumoral mRNA dosing appeared significantly enlarged with co-delivery of both cytokine and antigen mRNAs compared to either single group or control Scramble mRNA (Fig. 5b). Whereas frequencies of $CD8^+$ T cells in the tdLNs remained unchanged between any mRNA group, both the 5C and 5C + 3A groups displayed increased $CD4^+$ T cell numbers, memory $CD8^+$ T cell expansion, and enhanced T cell IFNγ expression in tdLNs (Fig. 5c–f). Impressively, dual cytokine and antigen mRNA (5C + 3A) administration led to significantly enhanced $CD8^+$ T cell effector differentiation, as well as induction of both $CD4^+$ and $CD8^+$ T cell proliferation and cytotoxicity, compared to antigen or cytokine mRNA dosing alone (Fig. 5g–j). Moreover, the 5C + 3A mRNA combination, but no other single or control mRNA arm, increased the frequency of TCF-1^+ stem-like $CD8^+$ T cells in the tdLNs that have been shown to be an important reservoirs for long-term anti-tumor T cells that can infiltrate "cold" TMEs and respond to ICB therapies[54] (Fig. 5k). In parallel, intratumoral

https://doi.org/10.1038/s41467-026-74574-z

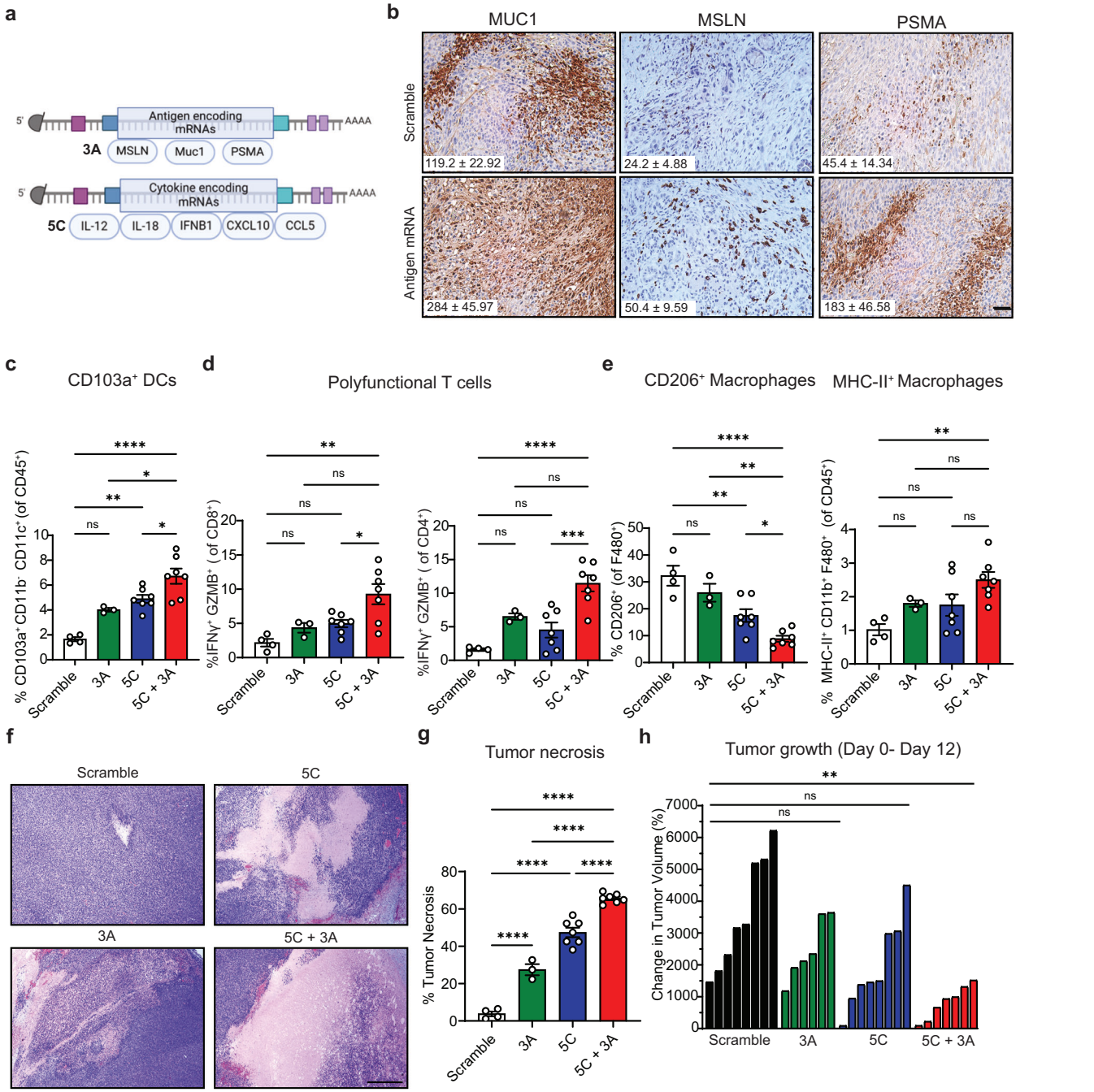

Fig. 4 | Combining cytokine with antigen-encoding mRNA delivery enhances antigen presentation and anti-tumor T cell immunity in "cold" PDAC model. **a** Schematic of the 3-antigen (3A) (MUC-1, MSLN, PSMA) and 5-cytokine (5C) (IL-12, IL-18, IFNβ, CCL5, CXCL10) mRNA cocktails. Created in BioRender. Ma, B. (2026) https://BioRender.com/eq52opy. **b** Representative IHC staining of *KPC1* orthotopic PDAC tumors from mice 24 h after intratumoral injection of either scramble mRNA (30 μg) or a 3-antigen mRNA cocktail (10 μg each of MUC-1, MSLN, and PSMA; 30 μg total). Scale bar, 100 μm. Quantification of the number of MUC-1$^+$, MSLN$^+$, and PSMA$^+$ cells per field is shown in the inset ($n = 5$ mice per group). Flow cytometry analysis of CD103a$^+$ cross-presenting DCs (**c**), polyfunctional IFNγ$^+$GZMB$^+$ T cells (**d**), and CD206$^+$ (M2) and MHC-II$^+$ (M1) macrophages (**e**) in *KPC1* orthotopic PDAC tumors on day 12 following intratumoral injections of either Scramble mRNA (80 μg), the 3A mRNA cocktail (10 μg each of MUC-1, MSLN, and PSMA; 30 μg total), the 5C mRNA cocktail (10 μg each of IL-12, IL-18, IFNβ, CCL5, and CXCL10; 50 μg total), or both 3A and 5C in combination every 3 days (Scramble, $n = 4$; 3A, $n = 3$; 5 C, $n = 7$; 5C + 3A, $n = 7$ mice). Data points for the Scramble and 5C groups in **c**–**e** are the same displayed in Fig. 2b, h and Supplementary Fig. 3k, m. **f** H&E staining of *KPC1* orthotopic PDAC tumors following 12 day treatment of mice as in **c**. Scale bar, 500 μm. Representative images of Scramble and 5C groups are the same displayed in Fig. 2k. **g** Quantification of the percentage of tumor area covered in necrosis from H&E staining in **f** (Scramble, $n = 4$; 3A, $n = 3$; 5C, $n = 7$; 5C + 3A, $n = 7$ mice). Data points for the Scramble and 5C groups are the same displayed in Fig. 2l. **h** Waterfall plot of the response of *KPC1* orthotopic PDAC tumors to 12 day mRNA treatment as in **c** (Scramble, $n = 8$; 3A, $n = 6$; 5C, $n = 8$; 5C + 3A, $n = 7$ mice). *P* values in **c**–**e** and **g**, **h** were calculated using ordinary one-way ANOVA with Tukey's correction. Data are presented as mean ± s.e.m. ns, not significant; $^*P < 0.05$; $^{**}P < 0.01$; $^{***}P < 0.001$; $^{****}P < 0.0001$. Source data are provided as a Source data file.

https://doi.org/10.1038/s41467-026-74574-z

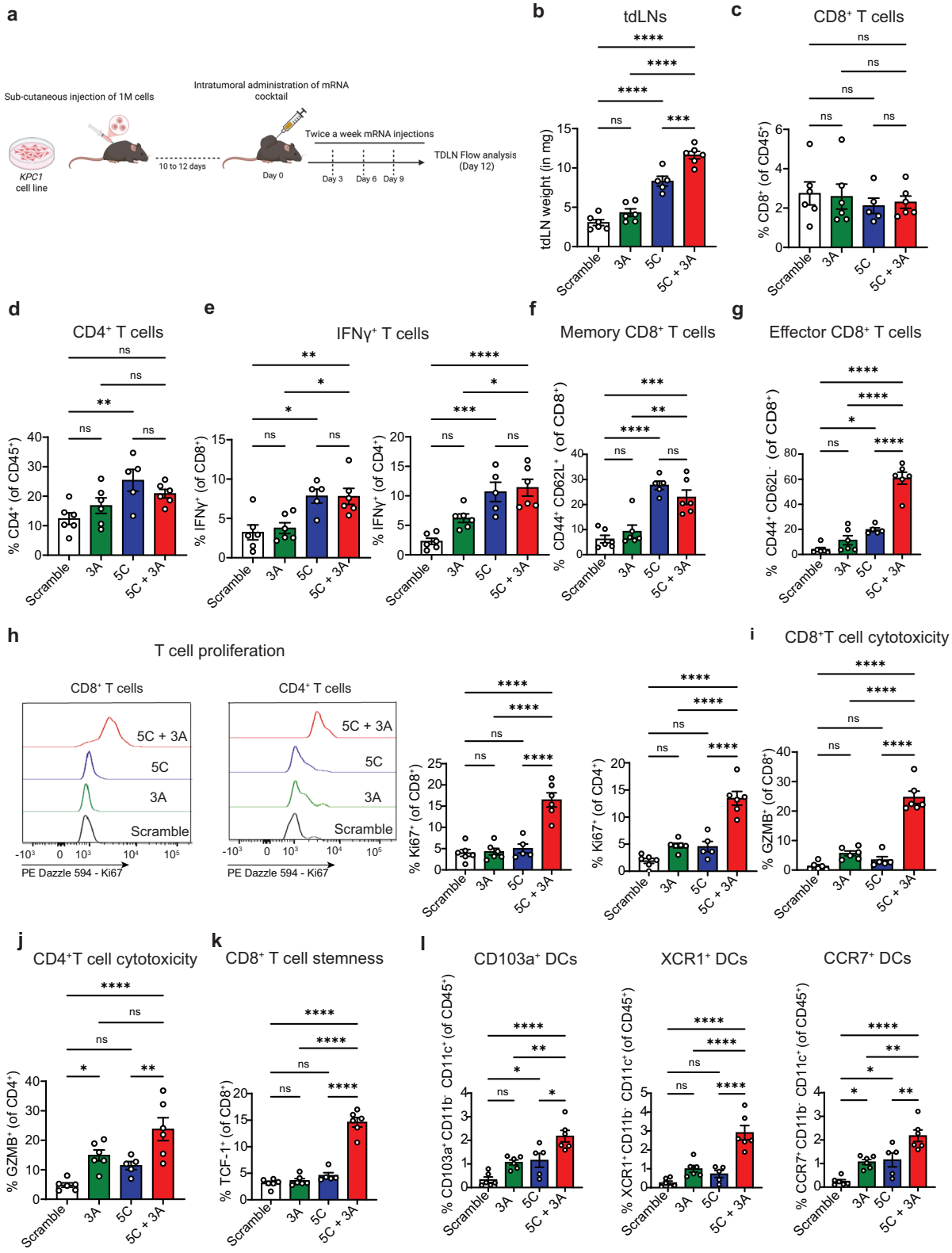

injection of the all-in-one cytokine and antigen mRNA cocktail resulted in the most significant increases in CD103a⁺ and XCR1⁺ DCs that cross-present antigens to and prime CD8⁺ T cells, as well as CCR7⁺ migratory DCs that chemotaxis between LNs and tumor sites compared to other treatment groups (Fig. 5l). Together, these findings demonstrate that combining antigen and cytokine mRNAs cooperatively enhances T cell proliferation, stemness, priming, and activation mediated by cross-presenting DCs within tumor-draining lymph nodes that likely contributes to sustained, long-term anti-tumor T cell responses to therapy.

A single dose of a multiplexed antigen and cytokine mRNA cocktail is sufficient to confer NK and CD8⁺ T cell-mediated PDAC control

Given the ability of cytokine and antigen mRNA co-delivery to mobilize stem-like and memory CD8⁺ T cell populations locally and systemically

Fig. 5 | Multiplexed cytokine and antigen mRNA delivery synergizes to sustain T cell proliferation, priming, and activation through enhanced DC antigen-presentation in the tumor-draining lymph nodes. a *KPC1* PDAC tumor cells expressing luciferase-GFP were subcutaneously injected into the right flank of 8- to 12-week-old female C57BL/6 mice. Following tumor establishment, mice received intratumoral injections of either Scramble mRNA (80 μg), the 3A mRNA cocktail (10 μg each of MUC-1, MSLN, and PSMA; 30 μg total), the 5C mRNA cocktail (10 μg each of IL-12, IL-18, IFNβ, CCL5, and CXCL10; 50 μg total), or both 3A and 5C in combination every 3 days. Tumor-draining lymph nodes (tdLNs) were harvested at Day 12 for flow cytometry analysis. Created in BioRender. Ma, B. (2026) https://BioRender.com/dheof59. **b** Weights of tdLNs (in mg) after 12 day treatment as in **a** (Scramble, $n = 6$; 3A, $n = 6$; 5C, $n = 5$; 5C + 3A, $n = 6$ mice). Flow cytometry analysis of $CD8^+$ (**c**) and $CD4^+$ T cells (**d**), $IFN\gamma^+$ $CD8^+$ and $CD4^+$ T cells (**e**), memory $CD8^+$ T cells (**f**), and effector $CD8^+$ T cells (**g**) in the tdLNs following repeated 12 day mRNA treatment of subcutaneous *KPC1* PDAC tumors as in **a** (Scramble, $n = 6$; 3A, $n = 6$; 5C, $n = 5$; 5C + 3A, $n = 6$ mice). **h** Representative histograms (left) and quantification of Ki67 expression in T cells (right) in the tdLNs following repeated 12 day mRNA treatment of subcutaneous *KPC1* PDAC tumors as in **a** (Scramble, $n = 6$; 3A, $n = 6$; 5C, $n = 5$; 5C + 3A, $n = 6$ mice). Flow cytometry analysis of cytotoxic $GZMB^+$ $CD8^+$ (**i**) and $CD4^+$ T cells (**j**), stem-like $TCF\text{-}1^+$ $CD8^+$ T cells (**k**), and $CD103a^+/XCR1^+$ cross-presenting and $CCR7^+$ migratory DCs (**l**) in the tdLNs following repeated 12 day mRNA treatment of subcutaneous *KPC1* PDAC tumors as in **a** (Scramble, $n = 6$; 3A, $n = 6$; 5C, $n = 5$; 5C + 3A, $n = 6$ mice). *P* values in **b**–**l** were calculated using ordinary one-way ANOVA with Tukey's correction. Data are presented as mean ± s.e.m. ns, not significant; $^*P < 0.05$; $^{**}P < 0.01$; $^{***}P < 0.001$; $^{****}P < 0.0001$. Source data are provided as a Source data file.

that can serve to sustain tumor-specific effector T cell responses long-term, we set out to determine if a single dose of an all-in-one cocktail containing 5 cytokine (IL-12, IL-18, CCL5, CXCL10, IFNβ) and 3 antigen (MSLN, MUC-1, PSMA) mRNAs would be sufficient to produce durable immune-mediated anti-tumor effects in our PDAC animal models (Fig. 6a). Flow cytometry analysis performed at an early 24 h timepoint following a single intratumoral dose revealed a significant increase in NK cell and DC frequencies, as well as NK and T cell polyfunctionality with 5C + 3A mRNA co-treatment (Fig. 6b–f), similar to the immunological effects observed with repeated cytokine and antigen mRNA dosing over 12 days. In contrast to the 12-day timepoint where no changes in total T cell numbers were observed, we found a significant increase in both $CD4^+$ and $CD8^+$ T cell frequencies 24 h after 5C + 3A mRNA therapy, suggesting an early wave of T cell recruitment in response to acute intratumoral mRNA delivery (Fig. 6g). However, there were no changes in macrophage or MDSC population dynamics at early timepoints, indicating that alterations in these myeloid populations is likely a secondary immunological effect occurring later on (Supplementary Fig. 7a, b). Together, these results demonstrate that our dual cytokine and antigen delivery approach is sufficient to activate NK and T cell immune responses in the PDAC TME in a rapid manner after a single dose.

Remarkably, a single intratumoral dose of the combined cytokine and antigen mRNA cocktail in established "cold" *KPC1* PDAC tumors led to a significant decrease in tumor growth 9 days post-treatment that culminated in prolonged overall survival outcomes compared to mice treated with control Scramble mRNAs (Fig. 6h, i). Though a single dose of the 5 cytokine mRNA mix on its own was also able to confer a survival benefit in PDAC-bearing animals, this survival advantage was significantly prolonged when combined with the 3 antigen mRNAs (Fig. 6i). To determine whether the observed anti-tumor effects of mRNA therapy were indeed immune-dependent, some mice that received the combined 3 antigen and 5 cytokine mRNA cocktail injection were also administered NK1.1 (PK136) or CD8 (2.43) monoclonal antibodies simultaneously to deplete NK cell and $CD8^+$ T cell populations, respectively (Supplementary Fig. 7c). Both NK and $CD8^+$ T cell ablation abrogated the survival benefit conferred by combinatorial cytokine and antigen mRNA therapy (Fig. 6j). Unexpectedly, depletion of NK, but not $CD8^+$ cells, blocked the anti-fibrotic effects of combined cytokine and antigen mRNA therapy, as evidenced by limited reduction in SMA^+ and $PDGFR\text{-}\beta^+$ myofibroblasts, FAP^+ activated CAFs, and collagen content following NK1.1 antibody treatment (Fig. 6k, l and Supplementary Fig. 7d–f). This highlights an underappreciated capacity of NK cells to target fibroblasts and resulting fibrosis that could further contribute to the anti-tumor and immune remodeling effects of cytokine/antigen therapy. Overall, these findings demonstrate that a single intratumoral dose of a combined cytokine and antigen mRNA cocktail is sufficient to orchestrate cytotoxic lymphocyte-mediated tumor suppression and fibrosis resolution, culminating in extended survival outcomes.

Systemic nanoparticle delivery of mRNAs achieves robust cytokine and antigen expression, local and peripheral immune responses, and PDAC growth control with minimal toxicity

As intratumoral (i.t.) injections of mRNAs could be challenging in patients with advanced PDAC where lesions may be multi-focal or otherwise inaccessible, we next evaluated the feasibility of encapsulating cytokine- and antigen-encoding mRNAs into pegylated lipid nanoparticles (NPs) to enable systemic delivery via tail vein injection. We successfully encapsulated the 5 cytokine mRNAs into NPs using ionizable lipids at high efficiency to produce an mRNA concentration (~10 μg per mRNA) comparable to our direct injection of free mRNAs (Supplementary Fig. 8a, b). These mRNA-loaded NPs also had a neutral charge and a small 50–60 nm diameter (Supplementary Fig. 8c, d), which we have previously shown to enable homing to and retention of NPs in the PDAC TME following systemic delivery with minimal toxicity and off-target inflammatory effects[14].

To assess NP biodistribution in vivo following systemic administration, DiI fluorescently labeled mRNA-loaded NPs were tracked across tissues in tumor-bearing *KPC1* transplant mice 24 and 48 h post-intravenous (i.v.) injection. As expected, the majority of fluorescent signal was detected in the liver where NPs passively deposit through the blood circulation at 24 h (Supplementary Fig. 8e, f). However, by 48 h, fluorescent NP signals in the liver were significantly reduced, while NP accumulation increased within PDAC tumors relative to the 24 h timepoint, indicating retention within the TME. Moreover, minimal fluorescent signal was detected in plasma, lung, or spleen at either time point, demonstrating rapid clearance from circulation and limited off-target distribution (Supplementary Fig. 8f). Flow cytometry analysis at 48 h revealed that NPs were taken up substantially more by both tumor and immune cells compared to stromal cells within the TME, with the highest uptake observed in DCs (Supplementary Fig. 8g).

We next compared i.t. administration of free mRNAs to i.v. administration of NP-encapsulated mRNAs head-to-head in *KPC1* orthotopic transplant models for their ability to induce cytokine and antigen expression in the PDAC TME. In tumors, i.t. delivery of the cytokine and antigen mRNA cocktail (5C + 3A) led to significant but transient increases in IL-12, IL-18, CCL5, IFNβ, and CXCL10 protein levels compared to Scramble control mRNAs, which peaked at 24 h and declined by 48 h (Supplementary Fig. 9a). In contrast, systemic NP-mediated mRNA delivery exhibited delayed kinetics, with minimal cytokine induction at 24 h followed by robust cytokine expression at 48 h after i.v. injection of the 5C + 3A cocktail (Supplementary Fig. 9a). Notably, with the exception of CXCL10, peak cytokine levels achieved at 48 h post-NP delivery significantly exceeded those observed at the 24 h peak following i.t. mRNA administration. I.t. mRNA delivery resulted in no induction of cytokines in the liver and blood aside from a transient increase in CCL5 in the liver at 24 h that reverted to baseline by 48 h (Supplementary Fig. 9b, c). While there was significant induction of the delivered 5C cytokines in the liver and blood 24 h after systemic NP mRNA delivery, by 48 h, cytokine concentrations largely

https://doi.org/10.1038/s41467-026-74574-z

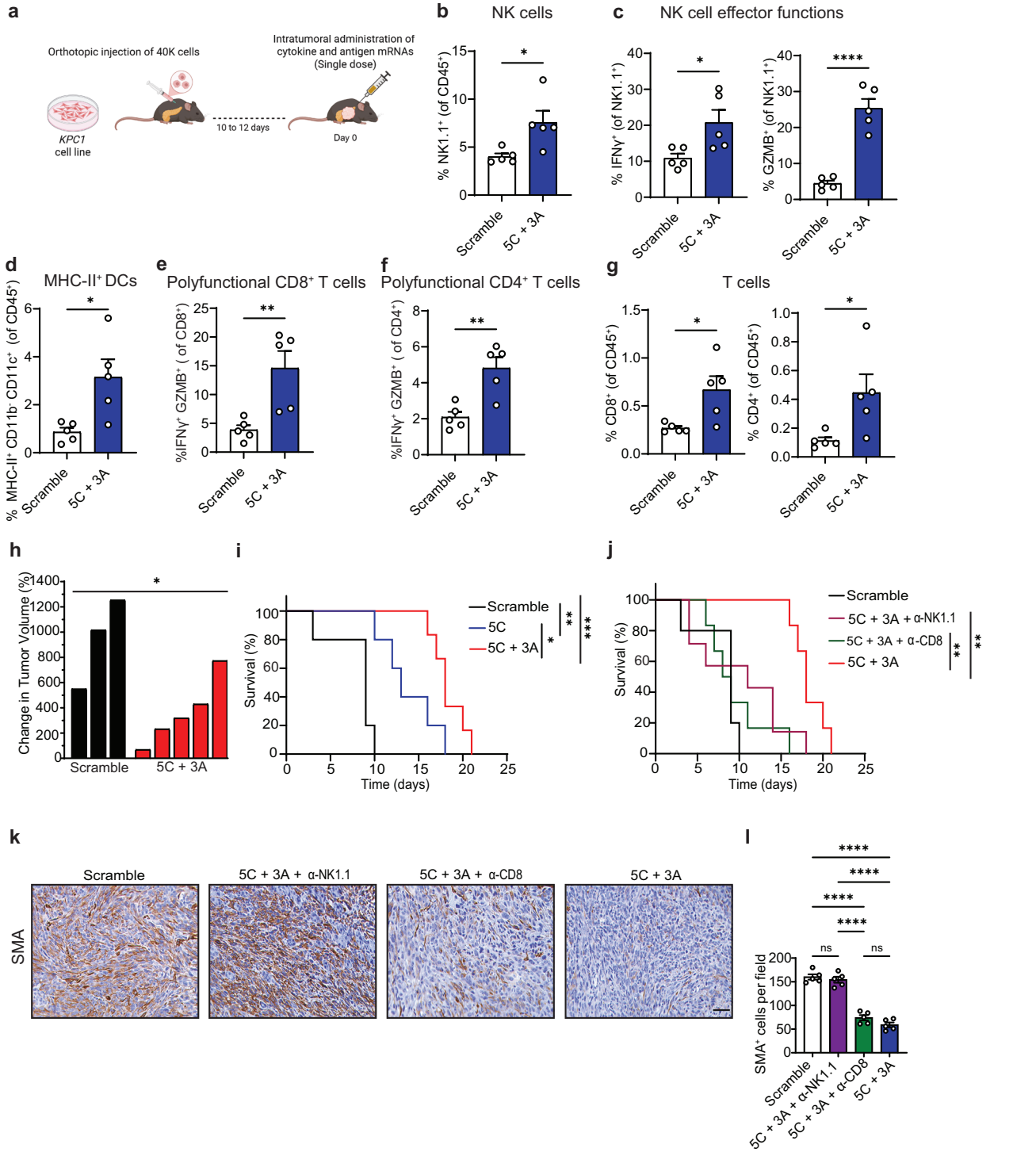

returned to baseline (outside of IFNβ and CCL5 in the liver) (Supplementary Fig. 9b, c). Both i.t. and systemic NP-mediated mRNA delivery of the 5C + 3A cocktail also led to an increase in expression of antigens MUC-1, MSLN, and PSMA in tumors 48 h post-injection compared to Scramble mRNAs, with NP delivery driving the highest frequency of antigen positivity (Supplementary Fig. 9d). ALT/AST levels in the blood and body weights were also measured following mRNA administration to assess liver and systemic toxicities. Whereas i.t. mRNA delivery did not alter ALT/AST concentrations in the blood, there was an increase in these liver enzyme levels at 24 h following NP-mediated i.v. delivery of cytokine and antigen mRNAs; however, this was transient, and ALT/AST levels reverted back to baseline by 48 h (Supplementary Fig. 9e). No significant body weight loss was observed with either the i.t. or i.v. delivery approach (Supplementary Fig. 9f). Together these data demonstrate that despite transient induction of cytokines systemically, i.v. delivery of NP-encapsulated mRNAs is able to effectively induce cytokine and antigen expression in the tumors to a similar, if not higher, degree than i.t. delivery of free mRNAs in a safe manner with minimal toxicity.

We also sought to determine the impact of different delivery routes and mRNA packages on local immune and tumor responses in the PDAC TME, as well as systemic immunity. Both i.t. and systemic NP delivery of the 5C + 3A mRNA combination led to substantial increases in $CD8^+$ and $CD4^+$ T cell and NK cell frequencies, as well as their

Fig. 6 | A single dose of an all-in-one antigen and cytokine mRNA cocktail is sufficient for NK and CD8⁺ T cell-mediated PDAC control. a *KPC1* PDAC tumor cells expressing luciferase-GFP were orthotopically injected into the pancreas of 8- to 12-week-old female C57BL/6 mice. Following tumor establishment, mice received a single intratumoral injection of either Scramble mRNA (80 μg) or the combined 5-cytokine (5C) and 3-antigen (3A) mRNA cocktail (10 μg each of IL-12, IL-18, IFNβ, CCL5, CXCL10, MUC-1, MSLN, and PSMA; 80 μg total). Mice were euthanized for downstream tumor analysis at 24 h. Created in BioRender. Ma, B. (2026) https://BioRender.com/mgz78r1. Flow cytometry analysis of NK cell frequencies (**b**), NK cell effector functions (**c**), DCs (**d**), polyfunctional IFNγ⁺ GZMB⁺ CD8⁺ (**e**) and CD4⁺ T cells (**f**), and total CD8⁺ and CD4⁺ T cells (**g**) in *KPC1* orthotopic PDAC tumors 24 h after a single dose of mRNA treatment as in **a** ($n = 5$ mice per group). **h** Waterfall plot of the response of *KPC1* orthotopic PDAC tumors to mRNA therapy 9 days after a single dose (Scramble, $n = 3$; 5C + 3A, $n = 5$ mice). **i**, **j** Kaplan–Meier survival curves of mice with *KPC1* orthotopic PDAC tumors treated intratumorally with a single dose of scramble mRNA (80 μg), the 5-cytokine mRNA cocktail (10 μg each of IL-12, IL-18, IFNβ, CCL5, and CXCL10; 50 μg total), or the combined 5-cytokine and 3-antigen mRNA cocktail (10 μg each of IL-12, IL-18, IFNβ, CCL5, CXCL10, MUC-1, MSLN, and PSMA; 80 μg total) in the presence or absence of NK1.1 (PK136; 250 μg) or CD8 (2.43; 200 μg) depleting antibodies (Scramble, $n = 5$; 5C, n = 5; 5C + 3A + a-NK1.1, $n = 7$; 5C + 3A + a-CD8, $n = 6$; 5C + 3A, n = 6 mice). Data points for Scramble and 5C + 3A groups are the same in **i** and **j**. **k** Representative IHC staining of *KPC1* orthotopic PDAC tumors at the survival endpoint following treatment as in **j**. Scale bar, 100 μm. **l** Quantification of SMA⁺ myofibroblasts per field from IHC analysis in **k** ($n = 5$ mice per group). *P* values in **b**–**h** were calculated using two-tailed, unpaired Student's *t*-test, and those in **l** were calculated using ordinary one-way ANOVA with Tukey's correction. *P* values in **i**, **j** were calculated using a log-rank test. Data are presented as mean ± s.e.m. ns, not significant; $^{*}P < 0.05$; $^{**}P < 0.01$; $^{***}P < 0.001$; $^{****}P < 0.0001$. Source data are provided as a Source data file.

expression of effector molecules IFNγ and GZMB in tumors compared to control Scramble mRNAs as assessed by flow cytometry analysis (Supplementary Fig. 10a–e). No significant changes in DC or macrophage numbers in the PDAC TME were observed with cytokine and antigen mRNA treatment through either delivery route at this early timepoint (Supplementary Fig. 10f, g). Interestingly, i.v. NP administration led to significantly higher T cell cytotoxicity as measured by GZMB positivity compared to i.t. delivery of 5C and 3A mRNAs (Supplementary Fig. 10c). 5C + 3A mRNAs could also achieve significant tumor growth reduction 48 h post-injection when administered systemically through NPs as opposed to i.t. delivery (Supplementary Fig. 10h). These enhanced immunological effects mediated through systemic NP delivery of mRNAs were also observed in peripheral organs. In the liver, whereas both delivery routes for cytokine and antigen mRNAs led to enhanced CD8⁺ T cell cytotoxicity, NK cell effector functions, and DC frequencies, only with i.v. NP delivery were increases in CD4⁺ and CD8⁺ T cell numbers and IFNγ expression, as well as NK cell and macrophage populations, observed (Supplementary Fig. 10i–o). In the spleen, both i.t. and i.v. administration of cytokine and antigen mRNAs led to increased CD8⁺ T cell, NK cell, and cytotoxic GZMB⁺ cell numbers as assessed by IHC staining of fixed tissues (Supplementary Fig. 11a, b). Still, this activation of cytotoxic lymphocytes in the spleen was significantly enhanced by systemic NP delivery as compared to i.t. 5C + 3A mRNA injections (Supplementary Fig. 11a, b). Importantly, despite immune activation in the liver and spleen, organ weights overall were not altered in any mRNA treatment group (Supplementary Figs. 10p and 11c). Few significant immunological changes were found in the blood, apart from augmented CD4⁺ T cell IFNγ expression, NK cell GZMB positivity, and DC frequencies with NP delivery of 5C + 3A mRNAs (Supplementary Fig. 11d–j). Collectively, these results showcase that systemic NP delivery of cytokine and antigen mRNAs can lead to superior immune activation and tumor control not only in the PDAC TME but also systemically in the liver and spleen that may further enhance long-term anti-tumor immune control.

NP-mediated delivery of cytokine and antigen mRNAs achieves long-term T cell immunity and curative tumor responses in an autochthonous PDAC mouse model

To further evaluate the therapeutic potential of our immunogenic cytokine- and antigen-encoding mRNA cocktail in a more clinically relevant setting, we expanded our studies into *KPC* genetically engineered mouse models (GEMMs) of PDAC that better recapitulate the development and histopathology of the human disease[55]. Given that *KPC* GEMMs develop spontaneous and multi-focal tumors throughout the pancreas that generally precludes direct intratumoral injection, we utilized our NP approach to deliver cytokine and antigen mRNA systemically. Similar to what we observed in *KPC1* PDAC orthotopic transplant models, while there was a transient spike in cytokine levels in the blood and liver 24 h following i.v. delivery of NPs loaded with the 5 cytokine mRNA cocktail into PDAC-bearing *KPC* GEMM mice, cytokine levels were mostly restored to baseline (with the exception of IFNβ in the liver and IL-18 in the blood) 48 h post-administration. In contrast, protein quantities of IL-12, IL-18, IFNβ, CCL5, and CXCL10 remained significantly elevated within PDAC tumors 48 h after i.v. injection of NPs encapsulated with the 5 cytokine mRNA cocktail compared to control Scramble mRNAs (Supplementary Fig. 12a–c). Moreover, systemic administration of NPs loaded with the 3 antigen mRNA cocktail also led to increased protein expression of MUC-1, MSLN, and PSMA in *KPC* GEMM PDAC lesions 48 h later as assessed by IHC analysis (Supplementary Fig. 12d). Importantly, i.v. administration of cytokine and antigen mRNA-encapsulated NPs led to no observable systemic toxicities as measured by changes in animal body weights or levels of liver enzymes ALT/AST up to 14 days post-treatment (Supplementary Fig. 12e, f). Thus, systemic administration of mRNAs through NP formulations is a safe and effective strategy to enhance cytokine and antigen expression in desmoplastic and hard-to-penetrate PDAC tumors in autochthonous GEMMs.

To assess the impact of NP-mediated cytokine and antigen mRNA delivery on immune and tumor responses in *KPC* GEMM tumors, we administered NPs containing the 5 cytokine and 3 antigen mRNA cocktails alone or in combination, or Scramble mRNA controls, by weekly i.v. injection following ultrasound confirmation of tumor formation (Fig. 7a). IHC analysis after 2-week treatment demonstrated increased accumulation of NKp46⁺ NK cells in the PDAC TME with both the 5 cytokine cocktail (5C) alone and in combination with antigens (5C + 3A) (Fig. 7b, c). Though 5C or 3A mRNAs individually led to an increase in total CD3⁺ and CD8⁺ T cells in the PDAC TME, 5C + 3A NP administration produced significantly higher CD3⁺ and CD8⁺ T cell infiltration compared to cytokine or antigen NP dosing alone (Fig. 7b, c). To more comprehensively profile the impact of cytokine and antigen mRNA therapy on innate and adaptive immune responses in autochthonous PDAC tumors, we performed flow cytometry analysis following treatment with mRNA NPs administered once weekly for two doses. Analysis confirmed increased numbers of CD8⁺ T cells and NK cells with combined 5C + 3A dosing, as was observed by IHC staining, as well as significantly enhanced CD4⁺ T cell, CD8⁺ T cell, and NK cell IFNγ and GZMB production and effector and memory CD8⁺ T cell differentiation (Supplementary Fig. 13a–h). In addition, combined cytokine and antigen mRNA NP dosing led to significant increases in antigen-presenting CD103a⁺ DCs and MHC-II⁺ macrophages along with a concomitant decrease in suppressive MDSCs (Supplementary Fig. 13i, j). Thus, an all-in-one cytokine and antigen mRNA cocktail can activate cytotoxic lymphocytes, mobilize antigen-presenting DCs, and remodel the immune suppressive myeloid landscape of the endogenous PDAC TME.

Further histopathological examination uncovered a striking ablation of adenocarcinoma pathology, with only rare tumor foci

https://doi.org/10.1038/s41467-026-74574-z

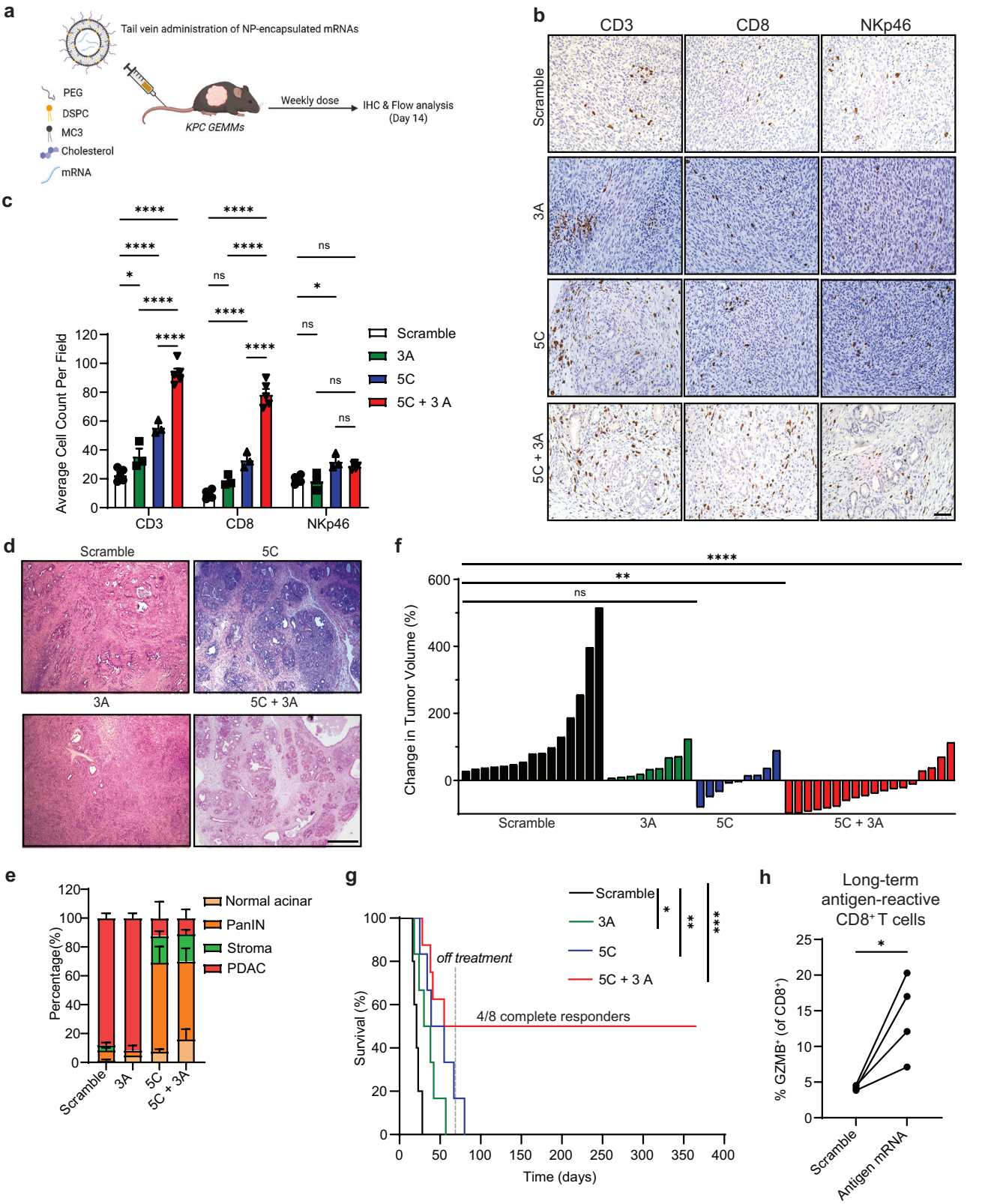

evident amongst predominantly normal acinar structures, pre-malignant pancreatic intraepithelial neoplasia (PanIN) lesions, and stroma in the pancreas of previously PDAC-bearing *KPC* GEMM mice treated with 5C or 5C + 3A mRNA NPs (Fig. 7d, e). This was in contrast to treatment with antigen or control Scramble mRNAs alone, which had no impact on tumor pathology in the pancreas (Fig. 7d, e). Though we did not observe increased areas of tumor necrosis as was seen with i.t. administration of 5C + 3A mRNA in *KPC1* orthotopic PDAC transplant tumors (Supplementary Fig. 13k), we found that systemic dosing of both cytokine mRNAs alone or in combination with antigen mRNAs in NPs could reduce the Ki67⁺ proliferation index in *KPC* GEMM tumors, as well an increase the number of dead/dying cleaved caspase-3⁺ cells that likely contribute to PDAC ablation (Supplementary Fig. 13l, m). Indeed, ultrasound imaging analysis after 2-week treatment

Fig. 7 | Systemic delivery of NP-encapsulated cytokine and antigen mRNAs produces curative tumor responses and long-term T cell immunity in autochthonous PDAC GEMMs. a *KPC* GEMMs with confirmed tumors received weekly intravenous (i.v.) injections of NPs encapsulated with scramble mRNA (80 μg), the 5-cytokine (5C) mRNA cocktail (10 μg each of IL-12, IL-18, IFNβ, CCL5, and CXCL10; 50 μg total), the 3-antigen (3A) mRNA cocktail (10 μg each of MUC-1, MSLN, and PSMA; 30 μg total), or combined 5C and 3A mRNA cocktails (80 μg total). Mice were either euthanized at Day 14 for IHC and flow cytometry analysis or treated until endpoint for long-term tumor growth and survival analysis. Created in BioRender. Ma, B. (2026) https://BioRender.com/ew4p4ax. **b** Representative IHC staining of *KPC* GEMM tumors 14 days after weekly mRNA NP dosing as in **a**. Scale bar, 100 μm. **c** Quantification of the number of $CD3^+$ T cells, $CD8^+$ T cells, and $NKp46^+$ NK cells per field from IHC analysis in **b** (Scramble, $n = 5$; 3A, $n = 3$; 5C, $n = 3$; 5C + 3A, $n = 5$ mice). **d** Representative H&E staining of *KPC* GEMM tumors 14 days after weekly mRNA NP dosing as in **a**. Scale bar, 500 μm. **e** Quantification of the percentage of normal acinar, stromal, pancreatic intraepithelial neoplasia (PanIN), and adenocarcinoma pathology in H&E stained sections of pancreas tumors from *KPC* GEMM animals treated for 14 days as in **a** (Scramble, $n = 4$; 3A, $n = 3$; 5 C, $n = 3$; 5C + 3A, $n = 5$ mice). **f** Waterfall plot of the response of *KPC* GEMM tumors to 14 day mRNA NP treatment as in **a** (Scramble, $n = 15$; 3A, $n = 9$; 5 C, $n = 9$; 5C + 3A, $n = 18$ mice). **g** Kaplan–Meier survival curve of tumor-bearing *KPC* GEMM animals treated weekly with mRNA NPs as in **a** (Scramble, $n = 5$; 3A, $n = 6$; 5C, $n = 6$; 5C + 3A, $n = 8$ mice). Dotted line indicates when mice were taken off treatment at Day 70. **h** Flow cytometry analysis of GZMB positivity in $CD8^+$ T cells derived from the blood of *KPC* GEMM animals with complete responses to 5C + 3A mRNA therapy 180 days after initial dosing and exposed to murine splenocytes primed with Scramble or antigen mRNAs (10 μg each of MUC-1, MSLN, and PSMA; 30 μg total) ex vivo ($n = 4$ mice per group). *P* values in **c** were calculated using two-way ANOVA with Tukey's correction. *P* values in **f** were calculated using one-way ANOVA with Dunnett's correction, and those in **g** using a log-rank test. *P* values in **h** were calculated using two-tailed, paired Student's *t*-test. Data are presented as mean ± s.e.m. ns, not significant; $^*P < 0.05$; $^{**}P < 0.01$; $^{***}P < 0.001$; $^{****}P < 0.0001$. Source data are provided as a Source data file.

revealed that both 5C and 5C + 3A mRNA groups, but not 3A alone, had significant PDAC tumor responses, with more frequent and substantial tumor regressions observed in the combined cytokine and antigen mRNA group (~72% of mice) compared to the 5C alone treatment arm (~33% of mice) (Fig. 7f).

Impressively, many of the PDAC tumors in mice treated with the all-in-one cytokine and antigen mRNA NPs continued to regress and even achieved complete responses as early as 8 weeks after repeated weekly NP dosing (Supplementary Fig. 13n). While PDAC-bearing *KPC* GEMM mice receiving control Scramble mRNA NPs quickly succumbed to the disease in a matter of weeks (median survival = 21 days), treatment with 3A or 5C single regimens was able to significantly extend survival by weeks (median survival = 34 and 47 days); however, mice still succumbed to their disease within 2–3 months (Fig. 7g). Remarkably, not only did treatment with combined 5C + 3A mRNA NPs dramatically extend the median overall survival by over 6 months (median survival = 210 days), but 50% of the *KPC* GEMM mice also had complete tumor responses (Fig. 7g). These complete responses were durable after treatment ceased, and were curative up to 1 year following initial mRNA dosing. To further assess the durability of antigen-specific immune responses in *KPC* GEMM mice that had been cured of pancreatic cancer following combined cytokine and antigen mRNA treatment, $CD8^+$ T cells were isolated from the blood 180 days after treatment initiation (110 days after treatment cessation) and evaluated for antigen reactivity ex vivo using antigen mRNA–pulsed splenocytes. Strikingly, circulating $CD8^+$ T cells still displayed cytotoxic responses when presented with antigen months after the last mRNA dose, suggesting long-lived, antigen-specific T cells that likely contribute to and help maintain complete tumor responses (Fig. 7h). Collectively, these results demonstrate that systemic delivery of a multiplexed cytokine and antigen mRNA therapy can achieve complete and curative tumor responses and long-term anti-tumor T cell immunity in autochthonous preclinical PDAC models.

Discussion

The PDAC TME is known to contribute to immune suppression and poor drug delivery, and as such, innovative strategies are needed to overcome these obstacles for effective immunotherapy[56]. Our previous work showed that therapies targeting the central KRAS signaling node in PDAC can remodel this immune suppressive TME through induction of the senescence-associated secretory phenotype (SASP), a collection of pleiotropic factors that include a diverse array of pro-inflammatory cytokines that are necessary to activate anti-tumor immunity and can potentiate ICB therapies[11,13,14]. However, senescent cell persistence and chronic SASP production can also conversely contribute to immune suppression and tumor progression through IL-6, IL-8, and other factors[57–60]. As such, we hypothesized that delivering only the cytokine signals we have shown to activate productive innate and adaptive immunity through the SASP, while bypassing the need for cellular senescence, could make for an effective immunotherapy for PDAC. To this end, we utilized mRNA technology to produce transient yet robust cytokine expression in the local PDAC TME through intratumoral delivery of SASP-related cytokine mRNAs. Given the modularity of mRNA synthesis, we were able to test different combinations of interleukins, chemokines, and interferons to fine tune the optimal combination to elicit DC, NK, and $CD8^+$ T cell mobilization and activation. A 5 cytokine cocktail consisting of IL-12, IL-18, CCL5, CXCL10, and IFNβ was able to fully activate NK cell immunity as well as generate polyfunctional $CD8^+$ T cells in "cold" PDAC mouse models compared to any single cytokine alone. Further combining the 5 cytokine mRNA cocktail with mRNAs encoding 3 known TAAs in PDAC could enhance DC antigen presentation and T cell priming and activation both in the TME and systemically. This all-in-one cytokine/antigen mRNA cocktail not only led to prolonged survival after just a single intratumoral dose in PDAC transplantation models but also produced curative tumor responses following weekly systemic administration of mRNA-loaded NPs in preclinical PDAC-bearing GEMMs. Thus, this multiplexed cytokine and antigen mRNA approach is capable of overcoming drug delivery limitations, reversing immune suppression, and activating long-term cytotoxic lymphocyte immunity to pave a path for an effective immunotherapy for PDAC.

Despite being one of the first FDA-approved immunotherapy modalities for cancer[17–20], cytokine therapies have traditionally relied on systemic delivery of single cytokine recombinant proteins that suffer from inflammatory toxicities and modest efficacy[21–25]. The ability to now synthesize cytokine-encoding mRNAs de novo with nucleoside modifications to enhance stability while reducing off-target inflammatory toxicities offers a means to safely induce multiple cytokines in the TME simultaneously. Indeed, intratumoral delivery of cytokine mRNA therapies can produce immune-mediated tumor regressions in "hot" melanoma models[26–28] and has even started to show promise in melanoma patients in early phase trials where it is well-tolerated (NCT03871348)[61]. However, whether cytokine mRNA therapies could also be effective in "cold" and immune suppressed PDAC tumors unresponsive to conventional immunotherapies is unclear. Recent studies showed that IL-12 mRNA could be delivered through intratumoral or intraperitoneal injection into mice with orthotopic PDAC lesions, leading to remodeling of myeloid-mediated immune suppression and activating T cell proliferation and effector functions[44,45]. Still, IL-12 mRNA therapy alone was not sufficient and required additional stereotactic body radiation therapy or anti-PD-1 immune checkpoint blockade in order to fully activate anti-tumor T cell responses in PDAC models. We also show that IL-12 mRNA treatment alone is sufficient to activate NK cell responses, DC antigen

presentation, and CD8⁺ T cell memory formation while reducing suppressive MDSC mobilization in "hot" but not "cold" PDAC models. Our work demonstrates that the effects of IL-12 mRNAs on immune suppressed TMEs can be potentiated when combined with mRNAs encoding other interleukins (IL-18), chemokines (CCL5, CXCL10), and interferon β. IL-18 contributed to further CD8⁺ T cell effector and memory formation, as well NK and CD4⁺ T cell cytotoxicity, CCL5 promoted NK cell chemotaxis and effector functions, and IFNβ enhanced tumor as well as DC antigen presentation, contributing to a multi-nodal adaptive and innate response with the 5 cytokine combination. IL-18 and CCL5 specifically led to a reduction in fibrosis in the PDAC TME, likely through their capacity to activate NK cells that we found to clear fibroblasts, revealing a novel secondary mechanism through which cytokine therapies could contribute to tumor suppression. Moreover, we found that delivery of these 5 cytokine encoding mRNAs leads to later induction of other cytokines, such as GM-CSF, important for DC activity, as well as chemokines CCL3, CCL4, and CXCL9, important for NK and T cell migration, which could further amplify the immune response. In the future, antibody-mediated depletion of delivered or induced cytokines could be used to tease out their relative contributions to anti-tumor immunity and to further optimize our mRNA cocktail for PDAC.

The addition of TAAs to our cytokine cocktail could further enhance polyfunctional CD4⁺ and CD8⁺ T cell activation, promote DC antigen presentation, and remodel suppressive macrophages within tumors. Strikingly, the combination of cytokine and antigen mRNAs was much more effective than either modality alone at mobilizing reservoirs of stem-like CD8⁺ T cells, as well as priming, expanding, and activating effector T cells through DC cross-presentation in the tumor-draining lymph nodes following intratumoral injections. Systemic delivery of cytokine/antigen mRNAs in NP formulations could likewise further enhance peripheral innate and adaptive immune activation in the liver and spleen. Mobilization of systemic immune responses in these secondary lymphoid organs likely contributes to a more robust and sustained anti-tumor immune response with cytokine and antigen mRNA therapy. Whereas cytokine and antigen mRNA combinations generated more significant tumor necrosis and enhanced overall survival compared to cytokine mRNAs alone when injected i.t. into *KPC* transplant PDAC models, only the all-in-one 5C and 3A cocktail administered through systemic NP delivery to *KPC* GEMM mice with autochthonous PDAC tumors was sufficient to ablate adenocarcinoma pathology and produce complete and curative tumor responses. Differences in the kinetics of tumor growth, baseline immune infiltration, stromal architecture, and mRNA delivery route and platform could explain differences in the degree and mechanism of tumor suppression observed between transplant and endogenous PDAC tumor models and will require further interrogation.

As antigen vaccines are typically delivered via intramuscular or subcutaneous injection to enhance DC uptake in the lymph nodes and systemic mobilization of T cell responses[62,63], it would be of interest to compare other delivery routes for our mRNA therapies, as well as different doses and treatment schedules. mRNAs themselves could also be further modified to enhance stability and protein production through use of circularized[64,65] or self-amplifying[66] RNAs, as well as formulated in hydrogels[67] to facilitate their slow release and retention in the TME. Similarly, NPs could be engineered with targeting peptides to not only increase their uptake in the tumor but possibly direct them to different cell types of interest in the TME to further increase potency while reducing systemic off-target effects. The modularity of our mRNA platform could allow us to multiplex other cytokines and antigens of interest, such as FLT3L[68] to expand DCs, IL-7 to further enhance T cell memory[69], or other putative TAAs in PDAC (e.g., EGFR[70], CLDN18.2[71], MUC16[72]) to target additional heterogeneous tumor cell populations. Incorporation of high-throughput single cell and spatial transcriptomic technologies to determine the effects of single or multiple cytokine and antigen combinations on specific immune subsets and T cell clones will provide a deeper understanding of the inflammatory mechanisms necessary to produce different types of immune responses to help further optimize these therapeutic approaches in PDAC and potentially across other cancer types[73,74].

Recently, neo-antigen RNA vaccines tailored to a patient's unique mutational profile have shown promising results in early phase trials in PDAC patients in combination with anti-PD-L1 ICB and chemotherapy regimens post-surgery[48], even resulting in persistent antigen-specific T cells peripherally in responders years later[49]. Our results suggest that multiplexed cytokine mRNA cocktails may serve as a potent adjuvant for antigen vaccines to further improve their efficacy by enhancing tumor and DC antigen presentation, promoting NK cell infiltration and cytotoxicity, remodeling immune suppressive myeloid populations, and potentiating T cell priming, effector expansion, and memory that are typically lacking in the majority of PDAC patients but yet required for durable anti-tumor T cell responses. Whereas mRNA-lipoplexes used in these neo-antigen vaccine trials home preferentially to the spleen of patients that are often removed during surgery, or amphiphile-modified KRAS vaccines used in other trials home to the lymph nodes[75], both our intratumoral as well as NP approaches direct cytokine and antigen signals to the PDAC TME to mediate local immune responses there. Moreover, while these vaccine trials treated patients with minimal residual disease post-surgery and in combination with other chemotherapy and immunotherapy regimens, we show that combined cytokine and antigen mRNA therapy can be used to treat established and treatment naïve tumors in preclinical PDAC models, leading to tumor ablation and curative responses in 50% of mice. As work from other groups has recently shown that TAAs may outnumber mutated neo-antigens and can provide durable antigen-specific immunity against PDAC and other tumor types[73,76], our platform using TAAs could offer an off-the-shelf approach to broaden the application of cancer vaccine strategies to more patients. Though not explored here, given that NPs deposit in the liver and promote immune activation there without toxicity following systemic delivery, it would be of interest to explore whether multiplexed cytokine/antigen mRNA therapy approaches could be used to target late-stage metastatic disease, which >50% of PDAC patients present with at initial diagnosis and typically in the liver. Collectively, our results put forward an all-in-one cytokine and antigen mRNA immunotherapy capable of producing complete tumor responses and long-term T cell immunity in preclinical PDAC models with clear translational relevance.

Methods

Ethical regulations

The research performed in this study complies with all ethical regulations. All mouse experiments were approved by the University of Massachusetts Chan Medical School Internal Animal Care and Use Committee (IACUC) (PROTO202000077).

mRNA synthesis and purification

Mouse cDNA sequences encoding IL-12p70 (p40p35) (Addgene; Cat. No. 108665; gift from Nevil Singh), IL-15 (OriGene; Cat. No. MR201274), IL-18 (OriGene; Cat. No. MR226935), IFNβ (OriGene; Cat. No. MR226101), CCL5 (OriGene; Cat. No. MG227153), CXCL10 (OriGene; Cat. No. MR200291), MUC-1 (OriGene; Cat. No. MR209607), MSLN (OriGene; Cat. No. MR209539), and FOLH1 (PSMA; OriGene; Cat. No. MR216035) were cloned into a pUC19 vector backbone (a gift from Dr. L. Li at UMass Chan) that includes a T7 promoter, 5′ UTR, 3′ UTR, and 110 bp poly A tail using Gibson Assembly (New England Biolabs; Cat. No. E5510S) according to the manufacturer's protocol. Sequences for the pUC19 vector backbone and cloned cytokine and antigen cDNAs are provided as Supplementary Sequences 1–10, and Gibson Assembly primers used for cloning listed in Supplementary Table 1.

cDNA containing pUC19 plasmids were then linearized downstream of the poly(A) signal using EcoRI restriction digestion (New England Biolabs; Cat. No R3101L). For synthesis and delivery of free (naked) mRNAs, in vitro transcription (IVT) was performed using T7 RNA polymerase (New England Biolabs; Cat. No E2050L) in the presence of a modified nucleotide mix, wherein uridine 5′-triphosphate (UTP) was substituted with N1-methylpseudouridine-5′-triphosphate ($m^1\Psi TP$) (TriLink; Cat. No N-1081-1) to enhance RNA stability and reduce immunogenicity. The IVT reaction also included ATP, CTP, and GTP at equimolar concentrations. Following transcription, the RNA was capped using a 7-methylguanosine (m^7G) cap analog (CellScript; Cat. No. C-SCCS1710) to ensure efficient translation. For synthesis of mRNAs to be encapsulated into lipid nanoparticles (NPs), IVT and post-transcriptional capping were performed using the mScript™ mRNA Production System (CellScript; Cat. No IMMY240625) according to the manufacturer's instructions. Scramble mRNA was synthesized from the pUC19-BNTns-EGFP vector lacking a start codon to prevent translation. A poly(A) tail (110 nt) was encoded in the DNA template to produce a polyadenylated transcript. The resulting capped and polyadenylated mRNA was purified using cellulose column chromatography to remove double-stranded RNA contaminants (Messenger Bio; Cat. No EMBARK100). Synthesized and purified IVT mRNAs were analyzed by electrophoresis on a 2% agarose gel stained with ethidium bromide to verify integrity and size. A single-stranded RNA ladder (ThermoFisher Scientific, Cat. No. SM1823) was included as a molecular weight reference.

mRNA lipid nanoparticle (NP) generation and characterization

mRNA NPs were synthesized via microfluidic co-flow focusing using a commercially available Fluigent Raydrop (1DPRD01). MC3 (48 mol% D-Lin-MC3-DMA, Cayman Chemical, 25325) and DSPC (10 mol% 1,2-distearoyl-sn-glycero-3-phosphocholine, Avanti, 850365C) were prepared in chloroform, along with 37 mol% cholesterol and 5 mol% DMG-PEG (1,2-dimyristoyl-rac-glycero-3-methoxypolyethylene glycol-2000, Avanti, 880151P), and formulations were dried overnight to form lipid films. Films were rehydrated in 200 proof ethanol. For microfluidic synthesis, mRNA stocks were diluted in sodium acetate buffer (pH = 3) at 20–200 μg/mL and used as the outer aqueous phase, and lipids rehydrated in ethanol were used as the inner organic phase in a microfluidic synthesis. The flow rates of the inner and outer phase were set to 12 μL/min and 72 μL/min, respectively. Following synthesis, mRNA NPs were dialyzed for 2 h against nuclease-free PBS. Dynamic light scattering (DLS) and zeta potential were used to measure NP hydrodynamic size and surface charge, respectively, using a Malvern Zetasizer. A commercially available mRNA detection kit (Quant-it RiboGreen, Invitrogen, R11490) was used to analyze loading capacity and encapsulation efficiency following dialysis.

Cell lines and compounds

Murine PDAC *KPC1* and *KPCY 2838c3* cell lines were generated from *KPC* and *KPCY* GEMM animals[11,47]. The *2838c3 KPCY* cell line was acquired from Dr. B. Stanger through an MTA with the University of Pennsylvania. *KPC1* cells were also engineered to express luciferase and GFP through retroviral transduction for tracking and visualizing in vivo[13]. Cancer-associated fibroblast (CAF) cell lines were isolated from PDAC tumors in *KPCY* mice by flow sorting for the YFP-negative fraction and confirmed to be fibroblasts by positive staining for SMA and negative staining for CK19 in culture. All cell lines were cultured in Dulbecco's Modified Eagle Medium (DMEM; Gibco, 11995073) supplemented with 10% fetal bovine serum (FBS; Sigma, F0926-500ML) and 100 IU/mL penicillin-streptomycin (P/S; Corning, 30-002-Cl), and maintained at 37 °C in a humidified incubator with 5% CO_2. *KPC1* cells were cultured on tissue culture dishes pre-coated with 100 μg/mL collagen (PureCol; Advanced BioMatrix, Cat. No. 5005). All cell lines tested negative for Mycoplasma contamination.

Trametinib (S2673) and palbociclib (S1116) were purchased from Selleck chemicals for in vitro studies. Drugs were dissolved in DMSO (vehicle) to yield 10 mM stock solutions and stored at −80 °C, and growth media with or without drugs were changed every 2–3 days.

mRNA transfection in vitro

Murine *KPC* PDAC cells, CAFs, and splenocytes were transfected with either scramble mRNA (2.5–3 μg) or cytokine-encoding mRNAs (0.5 μg each) using Lipofectamine MessengerMax reagent (ThermoFisher; Cat. No. LMRNA001), according to the manufacturer's instructions.

Animal models

All mouse experiments were approved by the University of Massachusetts Chan Medical School Internal Animal Care and Use Committee (IACUC). Mice were co-housed in a barrier facility, and food and water provided ad libitum. Housing conditions included a 12:12 light/dark cycle, with the lights coming on at 0700 and going off at 1900 daily, a temperature range of 20–26 °C, and a humidity range of 30–70%. C57BL/6 female mice were purchased from Charles River Laboratories (#027), and *P48-Cre* mice purchased from Jackson Laboratory (#023329). *P48-Cre; $Kras^{LSL\text{-}G12D/wt}$; $Trp53^{fl/wt}$* (*KPC*) GEMMs were generated by interbreeding *P48-Cre, $Kras^{LSL\text{-}G12D/wt}$* (Jackson Laboratory, #008179), and *$Trp53^{fl/fl}$* (Jackson Laboratory, #008462) strains on a C57BL/6 background. For tumor transplantation studies and ex vivo immune assays, only female C57BL/6 mice were used, as this greatly reduced costs and complications of housing adult male animals in the same cage. For studies using *KPC* GEMM mice, both male and female mice were used. Animal sex was not considered in the study design. Tumors did not exceed the maximum tumor size of 1500 mm^3 permitted by the University of Massachusetts Chan Medical School IACUC. To euthanize animals, mice were exposed to 100% carbon dioxide asphyxiation at 5 PSI for a minimum of 3 min, and death confirmed by palpating for the absence of an apex heartbeat and a lack of respiration.

Pancreatic orthotopic transplant models

Orthotopic pancreatic tumors were established by transplanting *KPC1* or *KPCY 2838c3* cells into the pancreas of 8- to 12-week-old female C57BL/6 mice. *KPC1* (4×10^4) or *KPCY 2838c3* (1×10^5) cells were resuspended in 25 μl of Matrigel (Corning, 354230) and diluted 1:1 with cold advanced DMEM/F12 medium (Gibco, 12634010). Mice were anesthetized using 2–3% isoflurane, and a small incision was made on the left flank to expose the pancreas. The cell suspension was injected into the tail region of the pancreas using a Hamilton syringe, and successful delivery was confirmed by the formation of a fluid bubble without leakage into the abdominal cavity. The abdominal wall was closed with absorbable Vicryl sutures (Fisher Scientific, 50-118-0848), and the skin was secured with wound clips (CellPoint Scientific Inc., 203-1000). Tumor induction and growth were monitored by ultrasound imaging. Once tumors formed (10 to 16 days after implantation), mice were randomized into treatment groups based on tumor volume. Upon euthanasia, pancreatic tumor tissue was separated for either fixation in 10% formalin for H&E and IHC staining, or digested into a single-cell suspension for flow cytometry analysis.

Subcutaneous transplant models

Subcutaneous pancreatic tumors were established by transplanting *KPC1* cells into the right flank of 8- to 12-week-old female C57BL/6 mice. *KPC1* (1×10^6) cells were resuspended in 50 μl of Matrigel (BD) and diluted 1:1 with cold PBS. Mice were anesthetized using 2–3% isoflurane, and cell suspension was injected into the right flank using a Hamilton syringe with successful delivery confirmed by the formation of a fluid bubble without leakage from the skin. Tumor induction and growth were monitored by caliper measurements. Once tumors formed (ten to twelve days after implantation), mice were randomized

into treatment groups based on tumor volume. Upon euthanasia, tdLNs were harvested and digested into a single-cell suspension for flow cytometry analysis.

KPC GEMMs

KPC genetically engineered mouse models (GEMMs) were generated by interbreeding *Trp53*$^{fl/fl}$, *Kras*$^{LSL\text{-}G12D/wt}$, and *P48-Cre* strains on a C57BL/6 background. Male and female *KPC* mice aged 3–6 months were used for all experiments. Tumor progression was monitored by ultrasound imaging, and mice were enrolled and randomized into treatment groups once tumors reached approximately 30 mm^3 in volume. Pancreas tumor tissue collected following euthanasia was fixed in 10% formalin.

Ultrasound imaging

High-resolution ultrasound imaging was conducted using the Vevo 3100 system equipped with an MS250 13–24 MHz transducer (VisualSonics). Imaging was performed to stage pancreatic tumors prior to randomization into treatment groups and to monitor tumor progression over time. Tumor volumes were quantified using Vevo LAB analysis software.

Intratumoral and systemic mRNA dosing in mice

For intratumoral mRNA delivery, single or combinatorial cocktails of free or NP encapsulated scramble, cytokine, and antigen mRNAs were injected directly into orthotopically or subcutaneously transplanted *KPC* tumors in mice (as verified by ultrasound imaging or caliper measurement) 10–16 days post-transplantation. Mice were lightly anesthetized with isoflurane to minimize movement during injection. One investigator gently palpated the abdomen to locate and stabilize the tumor near the surface of the skin, while a second investigator administered the mRNA formulation directly into the tumor through the skin using a Hamilton syringe. Fifty microliters of mRNAs diluted in Ringer's lactate (ThermoFisher; Cat. No. J67572.AP) at varying concentrations were delivered per injection. Care was taken to avoid leakage and ensure accurate delivery into the tumor mass. Mice received either a single injection or repeated twice weekly intratumoral injections. For systemic delivery of NP encapsulated mRNAs into *KPC* transplant or GEMM PDAC-bearing animals, mice received 200 μl intravenous tail vein injections of empty or mRNA loaded NPs containing ~10 μg of each mRNA weekly for 2 weeks or until survival endpoint. Ultrasound imaging was used to track tumor responses, and animal body weight changes and measurements of cytokine and AST/ALT levels in the blood and liver were used to monitor toxicity.

NK and CD8 depletion in vivo

For NK cell depletion, mice were administered intraperitoneal (i.p.) injections of an anti-NK1.1 antibody (250 μg; PK136, BioXcell; catalog no: BE0036) twice weekly. For $CD8^+$ T cell depletion, mice received i.p. injections of an anti-CD8 antibody (200 μg; 2.43, BioXcell; catalog no: BE0061) twice weekly. Effective depletion of NK and $CD8^+$ T cells was confirmed by immunohistochemical analysis of pancreatic tumor tissue.

Cytokine array

For in vitro cytokine array analysis, murine *KPC1* PDAC cells or CAFs were plated in six-well plates and either transfected with scramble or cytokine mRNA cocktails, or treated with trametinib (25 nM) and palbociclib (500 nM) (T/P). Twenty four hours post-transfection of mRNAs or 6 days post-treatment with T/P, conditioned media was collected, and cells were trypsinized and counted using a Countess II cell counter (Invitrogen). Media samples were then normalized to cell number by dilution with fresh culture media. A 75 μl aliquot of each sample was analyzed using the Mouse Cytokine/Chemokine 44-Plex or 36-Plex Discovery Assay Array (MD44 or MD36), or Mouse IL-18 Single Plex Discovery Assay Array (MDIL18) from Eve Technologies.

For cytokine array analysis of in vivo samples, tumor tissue, liver tissue, and blood were collected at different timepoints from *KPC* orthotopic transplant or GEMM animals following a single dose of free or NP formulated mRNAs delivered by intratumoral or intravenous injection. Tumor and liver tissues were mechanically dissociated using the MACS Dissociator (Miltenyi Biotec) prior to protein extraction. Total protein concentrations were quantified using the BCA kit (Bio-Rad; Cat. No 5000002). A total of 100 μl of each normalized sample was analyzed using the Mouse Cytokine/Chemokine 44-Plex or 36-Plex Discovery Assay Array (MD44 or MD36), or Mouse IL-18 Single Plex Discovery Assay Array (MDIL18) from Eve Technologies.

Systemic safety and tolerability

Liver, spleen, and blood were collected from mice with *KPC1* orthotopic transplant tumors 24 and 48 h after a single dose of free or NP formulated mRNAs via intratumoral or intravenous administration. Liver, spleen, and whole body weights were recorded to assess treatment tolerability. Plasma isolated from blood samples was analyzed for ALT and AST levels as a readout of hepatotoxicity by the UMass Chan Medical School Analytical Core. Similar analyses were also performed in PDAC-bearing *KPC* GEMM animals treated with NP-formulated mRNAs weekly for 2 consecutive weeks to determine long-term tolerability.

NP biodistribution analysis

To determine NP biodistribution, fluorescence imaging of DiI-labeled 5C + 3A mRNA NPs was performed on tumor tissues, blood plasma, livers, lungs, and spleens harvested from tumor-bearing *KPC1* orthotopic transplant mice 24 or 48 h after dosing ex vivo using an IVIS-Spectrum CT system (Perkin-Elmer). Quantification was performed using Living Image software, version 7.4.3.

NK and T cell migration assays

Primary NK cells and $CD8^+$ T cells were isolated from the spleens of 8- to 12-week-old female C57BL/6 mice using the NK Cell Isolation Kit II (Miltenyi Biotec; Cat. No 130-115-818) and $CD8a^+$ T Cell Isolation Kit (Miltenyi Biotec; Cat. No 130-104-075), respectively, according to the manufacturer's instructions. A total of 50,000 NK or $CD8^+$ T cells were diluted in serum-free DMEM supplemented with 100 IU/ml penicillin/streptomycin and seeded into the upper chamber of transwell inserts (Corning, 3422) placed in 24-well plates. Serum-free conditioned media collected 24 h post-transfection of *KPC1* tumor cells with single or combinatorial mRNA cocktails were added to the lower chamber. After 4 h of incubation at 37 °C in a humidified incubator with 5% CO_2, migrated cells in the lower chamber were fixed with 4% paraformaldehyde (PFA, ThermoFisher Scientific, J61899.AK), stained with DAPI (Millipore Sigma, D9542), and quantified using a Celigo imaging cytometer (Nexcelom).

NK and T cell co-culture assays

Primary NK and $CD8^+$ T cells were isolated from spleens of 8- to 12-week-old naïve female C57BL/6 mice using the NK Cell Isolation Kit II (Miltenyi Biotec; Cat. No 130-115-818) and $CD8a^+$ T Cell Isolation Kit (Miltenyi Biotec; Cat. No 130-104-075), respectively, according to the manufacturer's instructions. NK or $CD8^+$ T cells were then co-cultured at a 5:1 effector-to-target ratio with *KPC1* PDAC tumor cells transfected 24 h earlier with different single or combinatorial mRNA cocktails in RPMI media (Corning, 10-040-CV) supplemented with 10% FBS, PMA (20 ng/ml, STEMCELL Technologies, 74042), Ionomycin (1 μg/ml, STEMCELL technologies, 73722), and monensin (2 μM, Biolegend, 420701) in a humidified incubator at 37 °C with 5% CO_2. Following 4 h co-culture, IFNγ expression in NK and

$CD8^+$ T cells was assessed by flow cytometry analysis as described below.

Analysis of antigen-specific $CD8^+$ T cell responses ex vivo

To determine whether antigen mRNA vaccination could generate antigen-specific $CD8^+$ T cells in PDAC tumors, mice with orthotopically transplanted *KPC1* tumors were first injected intratumorally with scramble mRNA or a 3 antigen mRNA cocktail (10 μg each of MUC-1, MSLN, and PSMA; 30 μg total). Seventy-two hours after vaccination, $CD8^+$ T cells were purified from pancreatic tumor tissue using the $CD8a^+$ T Cell Isolation Kit (Miltenyi Biotec; Cat. No 130-104-075) according to the manufacturer's instructions. In parallel, splenocytes were harvested from naïve wild-type C57BL/6 mice and pulsed ex vivo with either scramble mRNA (3 μg) or antigen mRNAs (1 μg each of MUC-1, MSLN, and PSMA; 3 μg total) for 24 h. Antigen-pulsed splenocytes were then co-cultured with tumor-derived T cells at a 5:1 effector-to-target ratio for 4 h in RPMI media supplemented with 10% FBS, PMA (20 ng/ml, Sigma-Aldrich), Ionomycin (1 μg/ml, STEMCELL Technologies), and monensin (2 μM, Biolegend) in a humidified incubator at 37 °C with 5% CO_2. Antigen-specific T cell activation was assessed by flow cytometry analysis of IFNγ and GZMB expression as described below.

To evaluate long-term antigen-reactive $CD8^+$ T cell responses in vivo, peripheral blood was collected from *KPC* GEMM mice that achieved complete responses at day 180 post-treatment initiation (110 days after treatment cessation). $CD8^+$ T cells were isolated from blood (Miltenyi Biotec; Cat. No 130-104-075) and subjected to the same ex vivo co-culture assay with antigen-pulsed splenocytes as described above.

Clonogenic growth assays

Murine *KPC1* tumor cells or CAFs (5×10^5 cells) were seeded in six-well plates and transfected with either scramble or cytokine-encoding mRNAs. Seven days post-transfection, adherent colonies were fixed with a solution of 1% methanol and 1% formaldehyde, stained with 0.5% crystal violet (Fisher Scientific, C581-25), and imaged using a digital scanner (Epson perfection V500). To quantify colony formation, crystal violet–stained wells were solubilized in 100% ice-cold methanol, and absorbance was measured at 560 nm (OD_{560}) using a microplate reader (Promega Glomax, GM3000). Background signal from blank wells was subtracted to obtain final OD values.

To assess the impact of T/P treatment on durable senescence-associated growth arrest, *KPC1* tumor cells were first treated for 6 days with trametinib (25 nM) and palbociclib (500 nM) (T/P), and then replated in the absence of drugs. Adherent colonies were fixed with a solution of 1% methanol and 1% formaldehyde, stained with 0.5% crystal violet, and imaged using a digital scanner as above.

SA-β-gal staining

SA-β-gal staining was performed on *KPC1* tumor cells following 6 day T/P treatment. Cells were fixed with 0.5% glutaraldehyde in PBS for 15 min, washed with PBS supplemented with 1 mM $MgCl_2$, and stained for 6 h in PBS containing 1 mM $MgCl_2$, 1 mg/ml X-Gal (Invitrogen, 15520018), and 5 mM each of potassium ferricyanide and potassium ferrocyanide (at pH 5.5).

RT-qPCR

Total RNA was isolated from *KPC1* tumor cells using the RNeasy Mini Kit (Qiagen, Cat no. 74104). Complementary DNA (cDNA) was synthesized using the TaqMan reverse transcription reagents (Applied Biosystems, Cat no. N8080234) according to the manufacturer's instructions. Real-time qPCR was performed in triplicate using SYBR Green PCR Master Mix (Applied Biosystems, Cat no. 4385614) on the StepOnePlus Real-Time PCR system (Applied Biosystems, 015805). Gene expression values were calculated using the ΔΔCT method and normalized to *Gapdh* levels as an endogenous reference gene. Primer sequences for *Gapdh*: F, GCAGTGGCAAAGTGGAGATT; R, GAATTT GCCGTGAGTGGAGT. Primer sequences for *Cdkn2a*: F, AATCTCC GCGAGGAAAGC; R, GTCTGCAGCGGACTCCAT. Primer sequences for *Cdkn1a*: F, AGTTGGGTTCTGCTCCGTGGAG; R, ATCCCAACGCC CTGAACCGCT.

Immunohistochemistry

Formalin-fixed paraffin-embedded (FFPE) tissues were prepared by overnight fixation in 10% neutral-buffered formalin, followed by standard paraffin embedding and sectioning at 5 μm thickness. Hematoxylin and eosin (H&E), trichrome, and immunohistochemistry (IHC) staining were performed using established protocols. For IHC, tissue sections were deparaffinized, rehydrated through a graded ethanol series, and subjected to antigen retrieval by boiling in 10 mM citrate buffer (pH 6.0) or Tris EDTA (pH 9.0) for 15 min using a pressure cooker. Endogenous peroxidase activity was blocked with 3% hydrogen peroxide for 20 min, followed by two PBS washes.

Sections were incubated overnight at 4 °C with the following primary antibodies: CD3 (1:200; Abcam, ab5690), CD8 (1:100; eBioscience, 4SM15), NKp46 (1:100; R&D Systems, AF2225), Granzyme B (GZMB; 1:100; Abcam, ab4059), α-SMA (1:500; Abcam, ab5694), PDGFRβ (1:100; Cell Signaling Technology, 3169), FAP (1:100; Abcam, ab53066), Ki67 (1:100; Abcam, ab16667), Cleaved Caspase 3 (CC3) (1:200; Cell Signaling Technology, 9664), MUC-1 (1:200; Invitrogen, MA5-11202), Mesothelin (MSLN; 1:200; LS Bio, LS-C407883), and PSMA (FOLH1; 1:1000; Abcam, ab314142). The following day, sections were incubated with horseradish peroxidase (HRP)-conjugated secondary antibodies using the Vectastain Elite ABC-HRP kits specific to rat, rabbit, or goat IgG (Vector Laboratories; Cat. No.: MP-7444-15, MP-7401-50, and MP-7405-15, respectively) for 30 min. Signal detection was performed using 3,3′-diaminobenzidine (DAB; Vector Laboratories, SK-4105).

Stained sections were imaged using an Olympus BX41TF light microscope. Positive cells for each marker ($CD3^+$, $CD8^+$, $NKp46^+$, $GZMB^+$, SMA^+, $PDGFR\beta^+$, FAP^+, $MUC\text{-}1^+$, $MSLN^+$, $PSMA^+$, $Ki67^+$, and $CC3^+$) were quantified using ImageJ software by averaging counts from 5 to 10 randomly selected high-power fields (10× or 20× magnification) per tumor section. Tumor necrosis in transplanted PDAC models was assessed on H&E-stained sections by measuring the proportion of the total pancreatic tumor area composed of necrotic regions using ImageJ software. Collagen deposition in transplanted PDAC tumors was assessed on trichrome stained sections by measuring the proportion of the total pancreatic tumor area composed of collagen rich regions using QuPath software (0.7.0). Brightfield trichrome stained images were first color deconvoluted using the estimate stain vectors function on a representative region of tissue. Next, pixel classification was used to determine the total tissue area in each image and to quantify collagen area, with the threshold set according to the blue staining intensity of positive areas, with sigma smoothing applied to eliminate single positive pixels that may be present in non-collagen fiber areas. The percent collagen-stained area was calculated by dividing the collagen area μm^2 by the total tissue area μm^2 and multiplying by 100. Pathological assessment of pancreatic tumors in *KPC* GEMM animals following mRNA therapy was performed in a blinded manner by GI pathologist Dr. Zhen Zhao. The reported percentages represent best estimates based on pathologist assessment of whole slide images.

Flow cytometry analysis

To assess changes in surface MHC-I expression on *KPC1* cells cultured in vitro, cells were transfected with mRNAs and, where indicated, treated with an anti-IFNAR blocking antibody (10 μg/mL; BioXcell, BE0241) 24 h prior to analysis. Cells were then harvested by trypsinization, resuspended in PBS containing 2% FBS, and stained with

an anti-H-2K^b antibody (1:200; eBioscience, 12-5958-80) for 30 min on ice. Flow cytometry was performed on a FACSymphony A5 cytometer, and data were analyzed using FlowJo software (BD).

For in vivo analysis, pancreatic tumors, spleens, liver, tdLNs and/or blood were isolated from PDAC-bearing *KPC* transplant or GEMM animals treated with various mRNA formulations at indicated timepoints. Pancreatic tumors were then minced and enzymatically dissociated using the gentleMACS Octo Dissociator with heaters (Miltenyi Biotec) in collagenase buffer [1× HBSS with calcium and magnesium (Corning, 21-023-CV), 1 mg/ml collagenase V (Sigma, C9263-500MG), and 0.1 mg/ml DNase I (New England Biolabs, M0303L)] using the 37C_m_TDK1_1 program. Spleens were placed in 3 ml of PBS supplemented with 2% FBS in C tubes (Miltenyi Biotec, 130-096-334) and dissociated using program m_spleen_01 on a gentleMACS Octo Dissociator with heaters (Miltenyi Biotec). Liver tissues were isolated, minced, and enzymatically dissociated using the gentleMACS Octo Dissociator with heaters (Miltenyi Biotec) in collagenase buffer [1× HBSS with calcium and magnesium, 1 mg/ml collagenase IV (Sigma-Aldrich, C5138), and 0.1 mg/ml DNase I] using the 37C_m_LIDK2 program. tdLNs were isolated, minced, and enzymatically dissociated using the gentleMACS Octo Dissociator with heaters (Miltenyi Biotec) in collagenase buffer (1× HBSS with calcium and magnesium, 1 mg/ml collagenase IV, and 0.1 mg/ml DNase I) using the m_spleen_03 program. Following digestion, tissues were passed through 70-µm strainers, centrifuged, and resuspended in PBS + 2% FBS. Red blood cells were lysed using ACK lysis buffer (VWR, Cat no. 10128-806). Blood samples were centrifuged at 10,000 × *g* for 10 min to isolate plasma, which was collected and stored at −80 °C for downstream cytokine and metabolite analyses. The remaining cellular fraction was subjected to multiple rounds of ACK lysis prior to processing for flow cytometry analysis.

Single-cell suspensions were stained on ice for 30 min with the following antibodies (dilutions in parentheses): CD45 AF700 (1:320; BioLegend, 103128), CD11b BUV395 (1:1280; BD Biosciences, 565976), CD44 BV785 (1:100; BioLegend, 103059), CD62L PE-Dazzle 594 (1:200; BioLegend, 104447), NK1.1 BV605 (1:200; BioLegend, 108739), CD3 BV650 (1:300; BioLegend, 100229), CD8 PE-Cy7 (1:400; BioLegend, 100722), CD4 PE-Cy5 (1:200; BioLegend, 100410), CD11c BV785 (1:100; BioLegend, 117335), F4/80 APC (1:200; BioLegend, 123116), MHC-II PE (1:200; BioLegend, 107608), GR-1 PE-Dazzle 594 (1:200; BioLegend, 108451), CD103a BV711 (1:100; BD Biosciences, 748255), XCR1 BV605 (1:200; BioLegend, 148222), CCR7 PE-Cy7 (1:400; BioLegend, 120123), and CD206 BV650 (1:300; BioLegend, 141723). DAPI was used to exclude dead cells, GFP/YFP to mark transplanted *KPC1/KPCY* tumor cells, and DiI fluorophores to label NPs. Flow cytometry was performed using BD LSR II or FACSymphony A5 instruments, and data were analyzed using FlowJo software (BD). A representative flow cytometry gating strategy is shown in Supplementary Fig. 14.

For intracellular staining, single cell suspensions from in vivo tumor, liver, blood, spleen, and tdLN samples, or NK or CD8$^+$ cell ex vivo cultures, were incubated in RPMI-1640 supplemented with 10% FBS and penicillin/streptomycin, and stimulated with PMA (20 ng/ml), ionomycin (1 µg/ml), and monensin (2 µM) for 4 h at 37 °C. Surface staining was performed with CD45 AF700 (1:320; BioLegend, 103128), NK1.1 BV605 (1:200; BioLegend, 108739), CD3 BV650 (1:300; BioLegend, 100229), CD8 APC-Cy7 (1:200; BioLegend, 100714), and CD4 PE-Cy5 (1:200; BioLegend, 100410), followed by fixation and permeabilization using the Foxp3/transcription factor staining buffer set (eBioscience, 00-5523-00). Intracellular staining was conducted using GZMB APC (1:100; BioLegend, 515406), IFN-γ V450 (1:100; TONBO biosciences, 75-7311-U100), Ki67 PE-Dazzle 594 (1:200; BioLegend, 652427), and TCF-1 PE (1:200; BD Biosciences, 564217) antibodies. IFN-γ and GZMB expression were analyzed in CD3$^-$NK1.1$^+$ NK cells and CD3$^+$ CD4$^+$ or CD8$^+$ T cells. Ki67 and TCF-1 expression were analyzed in CD4$^+$ or CD8$^+$ T cells. A representative flow cytometry gating strategy is shown in Supplementary Fig. 14.

Statistics and reproducibility

Statistical analyses were performed as detailed in the corresponding figure legends. Data are presented as mean ± standard error of the mean (s.e.m.), with sample sizes (*n*) indicating biological replicates derived from independent samples. All samples meeting the appropriate experimental criteria were included in the analyses. Some mice were excluded from flow cytometry analysis if no grossly visible tumor was present, or from ultrasound tumor volume and immunohistochemical (IHC) analyses if tumors were predominantly necrotic. Mice that died prior to flow cytometry or ultrasound timepoints were also excluded. In vivo experimental groups were randomized to ensure comparable tumor burdens across groups, as determined by ultrasound imaging and caliper measurements. In vitro experiments were randomized at the sample allocation stage. No statistical methods were used to pre-determine sample sizes. Scoring of IHC staining in mouse tumor and spleen samples was performed in a blinded manner. Other experiments that were performed in real-time could not be blinded since researchers responsible for performing the experiments were involved in their design. All experiments were performed 2–3 times with similar results. Statistical significance was assessed using two-sided Student's *t*-tests, log-rank (Mantel–Cox) tests, or one- or two-way ANOVA followed by multiple comparison corrections (Tukey's, Dunnett's, or Sidák's), as appropriate. Analyses were performed using Prism 10 software (GraphPad). Data were assumed to follow a normal distribution, although this was not formally tested in all cases. A P value of <0.05 was considered statistically significant.

Reporting summary

Further information on research design is available in the Nature Portfolio Reporting Summary linked to this article.

Data availability

All data generated in this study are available in the figures, supplementary information, and source data files. Source data are provided with this paper.

References

1. Rahib, L., Wehner, M. R., Matrisian, L. M. & Nead, K. T. Estimated projection of US cancer incidence and death to 2040. *JAMA Netw. Open* **4**, e214708 (2021).
2. Siegel, R. L., Giaquinto, A. N. & Jemal, A. Cancer statistics, 2024. *CA Cancer J. Clin.* **74**, 12–49 (2024).
3. Ligorio, M. et al. Stromal microenvironment shapes the intratumoral architecture of pancreatic cancer. *Cell* **178**, 160–175.e27 (2019).
4. Olive, K. P. et al. Inhibition of Hedgehog signaling enhances delivery of chemotherapy in a mouse model of pancreatic cancer. *Science* **324**, 1457–1461 (2009).
5. Provenzano, P. P. et al. Enzymatic targeting of the stroma ablates physical barriers to treatment of pancreatic ductal adenocarcinoma. *Cancer Cell* **21**, 418–429 (2012).
6. Ohlund, D. et al. Distinct populations of inflammatory fibroblasts and myofibroblasts in pancreatic cancer. *J. Exp. Med.* **214**, 579–596 (2017).
7. Hilmi, M. et al. The immunological landscape in pancreatic ductal adenocarcinoma and overcoming resistance to immunotherapy. *Lancet Gastroenterol. Hepatol.* **8**, 1129–1142 (2023).
8. Li, X. et al. Immune checkpoint blockade in pancreatic cancer: trudging through the immune desert. *Semin. Cancer Biol.* **86**, 14–27 (2022).
9. Sharma, P. et al. Immune checkpoint therapy-current perspectives and future directions. *Cell* **186**, 1652–1669 (2023).

10. Cheng, N. C. & Vonderheide, R. H. Immune vulnerabilities of mutant KRAS in pancreatic cancer. *Trends Cancer* **9**, 928–936 (2023).
11. Ruscetti, M. et al. Senescence-induced vascular remodeling creates therapeutic vulnerabilities in pancreas cancer. *Cell* **181**, 424–441.e21 (2020).
12. Coppe, J. P. et al. Senescence-associated secretory phenotypes reveal cell-nonautonomous functions of oncogenic RAS and the p53 tumor suppressor. *PLoS Biol.* **6**, 2853–2868 (2008).
13. Chibaya, L. et al. EZH2 inhibition remodels the inflammatory senescence-associated secretory phenotype to potentiate pancreatic cancer immune surveillance. *Nat. Cancer* **4**, 872–892 (2023).
14. Chibaya, L. et al. Nanoparticle delivery of innate immune agonists combined with senescence-inducing agents promotes T cell control of pancreatic cancer. *Sci. Transl. Med.* **16**, eadj9366 (2024).
15. Dinarello, C. A. Historical insights into cytokines. *Eur. J. Immunol.* **37**, S34–S45 (2007).
16. Kureshi, C. T. & Dougan, S. K. Cytokines in cancer. *Cancer Cell* **43**, 15–35 (2025).
17. Rosenberg, S. A., Mule, J. J., Spiess, P. J., Reichert, C. M. & Schwarz, S. L. Regression of established pulmonary metastases and subcutaneous tumor mediated by the systemic administration of high-dose recombinant interleukin 2. *J. Exp. Med.* **161**, 1169–1188 (1985).
18. Kirkwood, J. M. et al. Interferon alfa-2b adjuvant therapy of high-risk resected cutaneous melanoma: the Eastern Cooperative Oncology Group Trial EST 1684. *J. Clin. Oncol.* **14**, 7–17 (1996).
19. Lotze, M. T. et al. High-dose recombinant interleukin 2 in the treatment of patients with disseminated cancer. Responses, treatment-related morbidity, and histologic findings. *JAMA* **256**, 3117–3124 (1986).
20. Rosenberg, S. A., Yang, J. C., White, D. E. & Steinberg, S. M. Durability of complete responses in patients with metastatic cancer treated with high-dose interleukin-2: identification of the antigens mediating response. *Ann. Surg.* **228**, 307–319 (1998).
21. Berraondo, P. et al. Cytokines in clinical cancer immunotherapy. *Br. J. Cancer* **120**, 6–15 (2019).
22. Siegel, J. P. & Puri, R. K. Interleukin-2 toxicity. *J. Clin. Oncol.* **9**, 694–704 (1991).
23. Wagstaff, J., Smith, D., Nelmes, P., Loynds, P. & Crowther, D. A phase I study of recombinant interferon gamma administered by s.c. injection three times per week in patients with solid tumours. *Cancer Immunol. Immunother.* **25**, 54–58 (1987).
24. Kurzrock, R. et al. Pharmacokinetics, single-dose tolerance, and biological activity of recombinant gamma-interferon in cancer patients. *Cancer Res.* **45**, 2866–2872 (1985).
25. Atkins, M. B. et al. Phase I evaluation of intravenous recombinant human interleukin 12 in patients with advanced malignancies. *Clin. Cancer Res.* **3**, 409–417 (1997).
26. Hewitt, S. L. et al. Durable anticancer immunity from intratumoral administration of IL-23, IL-36gamma, and OX40L mRNAs. *Sci. Transl. Med.* **11** https://doi.org/10.1126/scitranslmed.aat9143 (2019).
27. Hotz, C. et al. Local delivery of mRNA-encoded cytokines promotes antitumor immunity and tumor eradication across multiple preclinical tumor models. *Sci. Transl. Med.* **13**, eabc7804 (2021).
28. Hamouda, A. E. I. et al. Intratumoral delivery of lipid nanoparticle-formulated mRNA encoding IL-21, IL-7, and 4-1BBL induces systemic anti-tumor immunity. *Nat. Commun.* **15**, 10635 (2024).
29. Baiersdorfer, M. et al. A facile method for the removal of dsRNA contaminant from in vitro-transcribed mRNA. *Mol. Ther. Nucleic Acids* **15**, 26–35 (2019).
30. Svitkin, Y. V. et al. N1-methyl-pseudouridine in mRNA enhances translation through eIF2alpha-dependent and independent mechanisms by increasing ribosome density. *Nucleic Acids Res.* **45**, 6023–6036 (2017).
31. Kariko, K., Buckstein, M., Ni, H. & Weissman, D. Suppression of RNA recognition by Toll-like receptors: the impact of nucleoside modification and the evolutionary origin of RNA. *Immunity* **23**, 165–175 (2005).
32. Hingorani, S. R. et al. Preinvasive and invasive ductal pancreatic cancer and its early detection in the mouse. *Cancer Cell* **4**, 437–450 (2003).
33. Rhim, A. D. et al. EMT and dissemination precede pancreatic tumor formation. *Cell* **148**, 349–361 (2012).
34. Eksioglu, E. A., Mahmood, S. S., Chang, M. & Reddy, V. GM-CSF promotes differentiation of human dendritic cells and T lymphocytes toward a predominantly type 1 proinflammatory response. *Exp. Hematol.* **35**, 1163–1171 (2007).
35. Hamilton, J. A. & Anderson, G. P. GM-CSF biology. *Growth Factors* **22**, 225–231 (2004).
36. Dorner, B. G. et al. MIP-1alpha, MIP-1beta, RANTES, and ATAC/lymphotactin function together with IFN-gamma as type 1 cytokines. *Proc. Natl. Acad. Sci. USA* **99**, 6181–6186 (2002).
37. Romero, J. M. et al. A four-chemokine signature is associated with a T-cell-inflamed phenotype in primary and metastatic pancreatic cancer. *Clin. Cancer Res.* **26**, 1997–2010 (2020).
38. Romero, J. M. et al. Chemokine expression predicts T cell-inflammation and improved survival with checkpoint inhibition across solid cancers. *npj Precis Oncol.* **7**, 73 (2023).
39. Kariko, K., Ni, H., Capodici, J., Lamphier, M. & Weissman, D. mRNA is an endogenous ligand for toll-like receptor 3. *J. Biol. Chem.* **279**, 12542–12550 (2004).
40. Ryschich, E. et al. Control of T-cell-mediated immune response by HLA class I in human pancreatic carcinoma. *Clin. Cancer Res.* **11**, 498–504 (2005).
41. Pandha, H., Rigg, A., John, J. & Lemoine, N. Loss of expression of antigen-presenting molecules in human pancreatic cancer and pancreatic cancer cell lines. *Clin. Exp. Immunol.* **148**, 127–135 (2007).
42. Kasper, L. H. & Reder, A. T. Immunomodulatory activity of interferon-beta. *Ann. Clin. Transl. Neurol.* **1**, 622–631 (2014).
43. Mirlekar, B. & Pylayeva-Gupta, Y. IL-12 family cytokines in cancer and immunotherapy. *Cancers* **13** https://doi.org/10.3390/cancers13020167 (2021).
44. Hughson, A. L. et al. Integrating IL-12 mRNA nanotechnology with SBRT eliminates T cell exhaustion in preclinical models of pancreatic cancer. *Mol. Ther. Nucleic Acids* **35**, 102350 (2024).
45. Shen, Q. et al. Pancreas-targeted lipid nanoparticles for relatively non-invasive interleukin-12 mRNA therapy in orthotopic pancreatic ductal adenocarcinoma. *J. Control Release* **381**, 113588 (2025).
46. Karamitopoulou, E. Tumour microenvironment of pancreatic cancer: immune landscape is dictated by molecular and histopathological features. *Br. J. Cancer* **121**, 5–14 (2019).
47. Li, J. et al. Tumor cell-intrinsic factors underlie heterogeneity of immune cell infiltration and response to immunotherapy. *Immunity* **49**, 178–193.e7 (2018).
48. Rojas, L. A. et al. Personalized RNA neoantigen vaccines stimulate T cells in pancreatic cancer. *Nature* **618**, 144–150 (2023).
49. Sethna, Z. et al. RNA neoantigen vaccines prime long-lived CD8(+) T cells in pancreatic cancer. *Nature* https://doi.org/10.1038/s41586-024-08508-4 (2025).
50. Stromnes, I. M. et al. T cells engineered against a native antigen can surmount immunologic and physical barriers to treat pancreatic ductal adenocarcinoma. *Cancer Cell* **28**, 638–652 (2015).
51. Ciborowski, P. & Finn, O. J. Recombinant epithelial cell mucin (MUC-1) expressed in baculovirus resembles antigenically tumor associated mucin, target for cancer immunotherapy. *Biomed. Pept. Proteins Nucleic Acids* **1**, 193–198 (1995).
52. Ren, H. et al. Prostate-specific membrane antigen as a marker of pancreatic cancer cells. *Med. Oncol.* **31**, 857 (2014).

53. von Renesse, J., Lin, M. C. & Ho, P. C. Tumor-draining lymph nodes - friend or foe during immune checkpoint therapy?. *Trends Cancer* **11**, 676–690 (2025).
54. Connolly, K. A. et al. A reservoir of stem-like CD8(+) T cells in the tumor-draining lymph node preserves the ongoing antitumor immune response. *Sci. Immunol.* **6**, eabg7836 (2021).
55. Lee, J. W., Komar, C. A., Bengsch, F., Graham, K. & Beatty, G. L. Genetically engineered mouse models of pancreatic cancer: the KPC model (LSL-Kras(G12D/+);LSL-Trp53(R172H/+);Pdx-1-Cre), its variants, and their application in immuno-oncology drug discovery. *Curr. Protoc. Pharm.* **73**, 14 39 11–14 39 20 (2016).
56. Falcomata, C. et al. Context-specific determinants of the immunosuppressive tumor microenvironment in pancreatic cancer. *Cancer Discov.* **13**, 278–297 (2023).
57. Porciuncula, A., Hajdu, C. & David, G. The dual role of senescence in pancreatic ductal adenocarcinoma. *Adv. Cancer Res.* **131**, 1–20 (2016).
58. Zhou, L., Ma, B. & Ruscetti, M. Cellular senescence offers distinct immunological vulnerabilities in cancer. *Trends Cancer* **11**, 334–350 (2025).
59. Assouline, B. et al. Senescent cancer-associated fibroblasts in pancreatic adenocarcinoma restrict CD8(+) T cell activation and limit responsiveness to immunotherapy in mice. *Nat. Commun.* **15**, 6162 (2024).
60. Belle, J. I. et al. Senescence defines a distinct subset of myofibroblasts that orchestrates immunosuppression in pancreatic cancer. *Cancer Discov.* **14**, 1324–1355 (2024).
61. Bechter, O. et al. A phase I, first-in-human, dose-escalation, expansion trial of cytokine-encoding synthetic mRNA mixture alone or with cemiplimab in advanced solid tumors. *Clin. Cancer Res.* **31**, 2358–2369 (2025).
62. Moon, J. J. et al. Interbilayer-crosslinked multilamellar vesicles as synthetic vaccines for potent humoral and cellular immune responses. *Nat. Mater.* **10**, 243–251 (2011).
63. Liu, H. et al. Structure-based programming of lymph-node targeting in molecular vaccines. *Nature* **507**, 519–522 (2014).
64. Liu, C. X. et al. RNA circles with minimized immunogenicity as potent PKR inhibitors. *Mol. Cell* **82**, 420–434.e6 (2022).
65. Wesselhoeft, R. A., Kowalski, P. S. & Anderson, D. G. Engineering circular RNA for potent and stable translation in eukaryotic cells. *Nat. Commun.* **9**, 2629 (2018).
66. Comes, J. D. G., Pijlman, G. P. & Hick, T. A. H. Rise of the RNA machines - self-amplification in mRNA vaccine design. *Trends Biotechnol.* **41**, 1417–1429 (2023).
67. Zhong, R. et al. Hydrogels for RNA delivery. *Nat. Mater.* **22**, 818–831 (2023).
68. Maraskovsky, E. et al. Dramatic increase in the numbers of functionally mature dendritic cells in Flt3 ligand-treated mice: multiple dendritic cell subpopulations identified. *J. Exp. Med.* **184**, 1953–1962 (1996).
69. Bradley, L. M., Haynes, L. & Swain, S. L. IL-7: maintaining T-cell memory and achieving homeostasis. *Trends Immunol.* **26**, 172–176 (2005).
70. Nedaeinia, R., Avan, A., Manian, M., Salehi, R. & Ghayour-Mobarhan, M. EGFR as a potential target for the treatment of pancreatic cancer: dilemma and controversies. *Curr. Drug Targets* **15**, 1293–1301 (2014).
71. Woll, S. et al. Claudin 18.2 is a target for IMAB362 antibody in pancreatic neoplasms. *Int. J. Cancer* **134**, 731–739 (2014).
72. Haridas, D. et al. Pathobiological implications of MUC16 expression in pancreatic cancer. *PLoS ONE* **6**, e26839 (2011).
73. Ely, Z. A. et al. Pancreatic cancer-restricted cryptic antigens are targets for T cell recognition. *Science* **388**, eadk3487 (2025).
74. Cui, A. et al. Dictionary of immune responses to cytokines at single-cell resolution. *Nature* **625**, 377–384 (2024).
75. Pant, S. et al. Lymph-node-targeted, mKRAS-specific amphiphile vaccine in pancreatic and colorectal cancer: the phase 1 AMPLIFY-201 trial. *Nat. Med.* **30**, 531–542 (2024).
76. Apavaloaei, A. et al. Tumor antigens preferentially derive from unmutated genomic sequences in melanoma and non-small cell lung cancer. *Nat. Cancer* https://doi.org/10.1038/s43018-025-00979-2 (2025).

Acknowledgements

We thank B. Stanger from the University of Pennsylvania for providing *KPCY* cell lines and L. Li from UMass Chan for providing the pUC19 plasmid; G. Cottle for technical assistance; the UMass Metabolic Disease Research Center for performing analysis of blood metabolites in mice; the Morphology Core at UMass Chan Medical School for assistance with trichrome staining; and the Ruscetti and Pitarresi laboratories for helpful suggestions and comments on the manuscript.

Author contributions

C.N.P. and M.R. conceived the study, designed research, and wrote the manuscript with assistance from all authors; K.D.D., N.B., B.M., H.K.G., H.M., M.L.B., K.C.M., C.J., S.R., L.Z., L.C., K.H., and L.J.Z. designed, performed, and analyzed experiments. G.I.K., R.W.D., and P.U.A. synthesized NPs. Y.Q. and W.X. assisted with mRNA design and synthesis. Z.Z. provided histopathological analysis of tissue specimens. B.C.L. and J.R.P. provided intellectual input on the project. M.R. supervised the study.

Funding

This work was supported by funds from the Pancreatic Cancer Alliance to M.R. and J.R.P., NIH/NCI R00 awards to M.R. (CA241110) and J.R.P. (CA252153), and a Pancreatic Cancer Research Program (PCARP) Idea Development Award from the Department of Defense (DoD) to J.R.P. (PA230161P1). C.N.P. was supported by a fellowship from the Pancreatic Cancer Alliance and mRNA Research Advancement Award from CellScript. N.B. was supported by a Hopper-Belmont Inspiration Award and a postdoctoral fellowship from the Pancreatic Cancer Alliance. Z.Z. was supported in part by Developmental Funds from the Cancer Center Support Grant P30CA045508.

Competing interests

M.R. and J.R.P. are consultants for Boehringer Ingelheim. C.N.P., M.R., G.I.K., and P.U.A. have filed U.S. patent applications (Ser. Nos. PCT/US2025/031926 and PCT/US2026/030619) related to this work. C.N.P. and M.R. are also co-founders of ImmunoScript, Inc., a related biotechnology company. The other authors declare no competing interests.

Additional information

Supplementary information The online version contains supplementary material available at https://doi.org/10.1038/s41467-026-74574-z.

Correspondence and requests for materials should be addressed to Marcus Ruscetti.

Peer review information *Nature Communications* thanks Horacio Cabral who co-reviewed with Pengwen Chenand Helmut Friess for their contribution to the peer review of this work. A peer review file is available.